

Density Matrix Renormalization Group an Its Applications

A THESIS

submitted by

NISHANT GUPTA

for the award of the degree

of

MASTER OF SCIENCE



**DEPARTMENT OF PHYSICS
INDIAN INSTITUTE OF TECHNOLOGY MADRAS.**

April 2017

THESIS CERTIFICATE

This is to certify that the thesis titled **Density Matrix Renormalization Group and Its Applications**, submitted by **Nishant Gupta**, to the Indian Institute of Technology, Madras, for the award of the degree of **Master of Science**, is a bona fide record of the research work done by him under my supervision. The contents of this thesis, in full or in parts, have not been submitted to any other Institute or University for the award of any degree or diploma.

Prof. Suresh Govindarajan
Research Guide
Professor
Dept. of Physics
IIT-Madras, 600 036

Place: Chennai

Date: 21st April 2017

ACKNOWLEDGEMENTS

First of all I would like to thank my project guide Prof. Suresh Govindarajan for his invaluable guidance and supervision throughout the period of this project. The discussions with him were the constant source of inspiration and motivation.

I would like to thank my friends at IIT Madras for their constant support and encouragement.

I would also like to thank the developers of website sharelatex for providing an online platform to create and edit tex files without any hassle.

ABSTRACT

KEYWORDS: DMRG; Transverse Ising Model; Heisenberg Model

Density Matrix Renormalization Group has become an essential computational tool over the years to study condensed matter system in one dimension. Here we give a concrete review of the method and look at its applications in determining ground state properties of Transverse Ising Model and Heisenberg Model. We will also look for the signature of quantum phase transition with the help of entanglement entropy and various other observables defined on the system.

TABLE OF CONTENTS

ACKNOWLEDGEMENTS	i
ABSTRACT	ii
LIST OF FIGURES	v
1 INTRODUCTION	1
1.1 An Insight into Renormalization Technique	2
1.2 Wilson Renormalization Method and why it fails?	4
2 Density Matrix Renormalization Group	6
2.1 Infinite DMRG Algorithm	6
2.2 Finite DMRG Algorithm	11
2.3 Singular Value Decomposition and Schmidt Decomposition	13
2.4 Why DMRG works?	15
2.5 Measurement of Observables and Ground state properties	16
3 Transverse Ising Model	21
3.1 Formation of superblock in Transverse Ising Model	21
3.2 Numerical Results	23
4 XXZ Heisenberg Model	36
5 Conclusions and Outlooks	41

LIST OF FIGURES

2.1	This figure shows the iterations taken in infinite system DMRG. New blocks are formed by integrating a site into a block. These blocks combine to form superblock and the new block has a truncated state space due to density matrix formulation. The growth happens on both the side leading to the chain growth (Schollwöck, 2011).	9
2.2	This figure shows the iterations taken in finite system DMRG. It starts from where Infinite DMRG ends. New blocks are formed by integrating a site into a block. These blocks combine to form superblock and the new block has a truncated state space due to density matrix formulation. Unlike Infinite DMRG growth happens only for one side at the expense of the other leading to constant chain length (Schollwöck, 2011).	12
3.1	Plot of Energy dependence on the system size calculated with Infinite DMRG upto 100 sites with $m = 30$. We can see that energy falls very sharply at the initial sizes but then attain a slow gradual decline . . .	24
3.2	Plot of energy difference of ground state vs the system size for various number of basis states kept in infinite DMRG. The dashed line and horizontal dashed line is the difference in the ground state energy for 5 and 30 basis states kept and 5 and 40 basis states kept respectively, the solid line and circles represents the difference in the ground state energy of Infinite DMRG with 20 and 40 basis kept and 20 and 30 basis kept. Total number of sites are 50.	25
3.3	This plot shows how energy changes with each step of finite DMRG. No of site is 20 and we start from the middle of the block. For few steps energy is changing before taking on a constant value for left block. The right block then starts growing having the same constant energy when it reaches in middle and from there energy starts to decrease again till it reaches the final converged value at 20th iteration after which it does not change in later sweeps.	26
3.4	Entanglement Entropy Vs the system size during each step of Infinte DMRG upto 50 sites.	27
3.5	Entanglement Entropy of the subsystem of different sizes using finite DMRG within the total length of 50, 100 and 200 sites keeping $m=30$	28
3.6	Ground state energy vs h_x/J for 50, 100 and 200 sites keeping $m=30$	29
3.7	Order parameter variation with transverse magnetic field for 50 sites without any bias	29

3.8	Order parameter for 100 sites with respect to transverse magnetic field for $m=30$ with an external bias magnetic field in longitudinal direction applied to the Hamiltonian.	30
3.9	Mass gap variation with J/h_x for various system sizes. For $J/h_x < 1$ is a paramagnet phase and near the phase transition mass gap goes to zero and system becomes gapless.	31
3.10	Entanglement Entropy with respect to J/h_x	32
3.11	Von Neumann entropy and Rényi entropy for $k=2,3,4$ for 100 sites. When $k \rightarrow 1$ Rényi entropy collapses onto Von Neumann entanglement entropy	33
3.12	Plot of one point correlation function $\langle S_z \rangle$ with respect to J/h_x at site 96 and 47. $g = h_x = 1$	34
3.13	Two point correlation function of $\langle S_z \rangle$ for two different sites on a 200 sites lattice.	35
3.14	Two point correlation function of $\langle S_x \rangle$ for two different sites on a 200 sites lattice.	35
4.1	Ground state variation with Δ for a lattice having 50 sites. The reduced basis state number $m=40$	37
4.2	Plot of Entanglement Entropy at the centre of chain at every finite DMRG step vs the block size. The reduced basis states is $m=40$. . .	38
4.3	Plot for the variation of mass gap of Hiesenberg Model with Δ for a lattice of 26 sites. The reduced basis state number is $m=40$	38
4.4	Order parameter variation with Δ for a lattice having 50 and 100 sites. The reduced basis state number is $m=40$. The red and blue circles are for 50 sites and diamonds are for 100 site. Here $h_z = h_{\text{stagg}} = 1.8$	40

CHAPTER 1

INTRODUCTION

Quantum Many Body Physics is the field which is used to study the dynamics and interaction of many particle system. Our main focus in this thesis are on strongly correlated quantum systems on low dimensional lattices mainly one dimension. Many Quantum lattice models are probed in one dimension where we study quantum phase transition, correlation effects in these quantum spin models. These observations than provide great insights in the behaviour of these interacting systems in higher dimension. Hence we can say that studying these systems in one dimension is very important in theoretical condensed matter physics. However both analytically and numerically it is a big task to accomplish. Several theoretical techniques like perturbation theory fails in presence of strong interaction and other techniques are not fully equipped to completely solve the problem and require the assistance of numerical methods like Monte Carlo simulation, series expansions and exact diagonalisation.

Now in general for any many body problem, the main issue is dealing with large Hilbert Space, even for spin $1/2$ particles on a lattice the dimension of Hilbert space grows exponentially and is equal to 2^N where N is the total number of sites on the lattice. A lot of numerical and computational resources then go into storing observables (Hamiltonian, order parameter) with large matrix dimension and solving them. This has been one of the main challenges in computational methods and therefore it becomes of utmost importance that a way or procedure is developed to tackle this problem. We can take hints from Quantum field theory and statistical mechanics where the theory of Renormalization was proposed to deal with systems having very large degrees of freedom. Kadanoff blocking employed on lattice models is one such example. Essentially what we can do is truncate the Hilbert space so that very minuscule information or no information is lost while calculating various properties associated with our lattice model. In comes Density Matrix Renormalization Group(DMRG) which is a very excellent way to find the ground state energy and properties of various lattice systems in

1D and since its inception it has seen lot of success. It was developed as an improvement over Wilson Renormalization Group which is discussed in detail in later sections. Using the concept of reduced density matrix for a block having few sites embedded in a very long chain it systematically truncates the Hilbert Space to a much smaller and manageable dimension that is easy to work without losing any information and capturing the essence of all the properties attributed to the ground state and few low lying excited states of the system.

In the section on DMRG we have given the answers as to why this whole ordeal of truncation of Hilbert space will work? The answer emerges from the discussion of entanglement entropy and how it scales with system size but before we proceed to that we need to go through an overview of renormalization where we briefly mention the historical context and techniques involved in it.

1.1 An Insight into Renormalization Technique

During the advent of Quantum Electrodynamics field theorists encountered Ultraviolet divergences in QED diagrams while computing for radiative correction and therefore to eliminate these infinities from the theory Renormalization technique was created. We restrict the integral to some ultraviolet cut off Λ and rescale the parameters in the theory such that the final amplitude for radiative correction is finite when $\Lambda \rightarrow \infty$. It is a way to study physics at different length scales. Not long after the technique was invented it was realised that the implications of Renormalization method were far reaching in the scaling theory of critical phenomena.

Before Renormalization method came into picture it was known that near critical point various thermodynamic quantities show scaling behavior for example free energy \mathcal{G} can be written as the homogeneous function of h and t

$$G = |t|^{\Delta+\beta} \mathcal{G}_{\pm}(h/|t|^{\Delta}) \quad (1.1)$$

where $t = \frac{T-T_c}{T_c}$, T_c being the critical temperature of the system, β is the critical exponent, Δ is the mass gap and h is the external magnetic field (Huang, 1987). At critical temperature the correlation length which is the only length involved in the system goes

to infinity and therefore one has microscopic fluctuation at all length scales from 1 \AA upto correlation length which tends to infinity. This is one of the reason why phase transition is such an interesting phenomena where unexpected behavior occurs. Most theoretical methods are not equipped for handling fluctuations and they fail since they cannot accommodate all the possible scales. Landau approached this problem by taking a coarse grained order parameter density $m(x)$ and defined it such that there is no fluctuation in $m(x)$ with wavelength smaller than an atomic distance a , correspondingly $m(x)$ may not have wavenumber greater than cutoff $\Lambda \sim 1/a$. The effective Hamiltonian is proportional to the functional of $m(x)$ and H and is given by

$$E = \int d^d x \psi(m(x), H) \quad (1.2)$$

where $\psi(m(x), H)$ is 'landau free energy' which is a function of higher order of $m(x)$ and its derivatives. The integration extends over all the possible fluctuation of $m(x)$ which do not vary over an atomic distance a . To have a complete macroscopic theory Λ must vanish from all the physical answers. Since $1/\Lambda$ is of microscopic scale therefore we take $\Lambda \rightarrow \infty$ which will produce divergence in the free energy. The correct procedure for taking such a limit involves renormalization. In spatial dimension less than 4, Gaussian model for Landau free energy suggests that long wavelength fluctuations dominate critical properties of the system.

This means that we can continue the coarse graining procedure (averaging out the details on small atomic scales) by throwing away irrelevant degrees of freedom and that is what Kadanoff did when he implemented his idea of block spin transformations on the Ising model which in short rightly assume that near the critical point the spins should act in same harmony in large blocks. Thus the important degree of freedom becomes the average spins of the blocks, rather than the original individual spins. One should then describe the system in terms of an effective Hamiltonian involving only these "block spins" and have a system in hand which has lesser degrees of freedom. This way one can see how various parameters (coupling constant, magnetic field) changes during each spin block transformation and at the critical temperature the parameters attain a fixed value and they stop changing and thus our system becomes scale invariant. Kadanoff's model was simple and although his idea was brilliant but it made too many assumptions which were wrong such as the interaction between neighbouring blocks only when clearly blocks can have more complicated interactions than that. In 1971 Kenneth Wil-

son presented his work on Renormalization Group(RG) (Wilson, 1975). The operation of coarse-graining followed by rescaling is called a renormalization-group (RG) transformation. In momentum space it translates to integrating out portion of momentum space say from some Λ to Λ/b where $b > 1$ of a Hamiltonian E and then rescale it back by increasing the unit of length b and restoring the cutoff to Λ . This modify coupling constants so that Hamiltonian has the same functional form, the change in coupling constants results in a differential equation under RG transformation which we can solve to get the fixed points of the system.

1.2 Wilson Renormalization Method and why it fails?

In this section Wilson RG method will be described in context of 1D lattice model (White and Noack, 1992). Here are the steps for how it works

1. First of all we consider a lattice model for N sites whose ground state properties we are interested in . Now in that chain label a block B containing few sites, lets say k sites (minimum two). Then we form a Hamiltonian for block B and diagonalize it.
2. After diagonalizing it we choose m (or any other number of prefixed basis states) lowest energy eigenvalues and their corresponding eigenstates v_i and form a matrix ' O ' of $l \times m$ dimension with v_i 's as column vectors where $l = 2^k$.
3. Now we change the basis and truncate all the operators defined on block B , getting new block B' by performing the following transformation

$$H' = O^T . H . O \quad S_i^{z'} = O^T . S_i^z . O$$

the matrix H defined on block B has dimensions of $l \times l$ and matrix H' defined on block B' has the dimensions of $m \times m$ and similarly for S_i^z . This way we have restricted the dimension of operators defined on a new block to the given m basis states.

4. Next we connect two adjacent block B' 's each with the basis sates m to give a resultant basis state m^2 and label this block with B'' . The Hamiltonian on this block is defined as

$$H'' = H' \otimes I + I \otimes H' + S_i^z \otimes S_{i+1}$$

where I is a unit matrix of dimension $m \times m$ defined on the neighbouring block. The third term in the above expression is a connecting term where each S^z is

defined at the end of one block and at the beginning of the neighbouring block. The dimension of H'' then becomes $m^2 \times m^2$

5. We then proceed as in step (3) to truncate and change the basis of all the operators defined on B'' and the whole step (4) is repeated again until we have covered every site on the lattice.

The whole idea in a nutshell is that the higher energy states which are thrown away at each step (3) are unimportant and does not have any contribution in determining the ground states and few low energy states. We can increase accuracy by keeping more states. The application of this approach to a 1D tight binding lattice fails drastically because of the boundary conditions used by the approach. The block is treated as isolated from the rest of the system and the boundary conditions are fixed at the edges of the block which means that the eigenstates of the block vanish at the edge. Therefore block B'' formed from two B' block in the step (iv) will have a kink in the middle as fixed boundary condition is used in the two initial blocks and any set of truncated states will be in some sense insufficient and will give large truncation error. This problem can be rectified to a great extent by combining eigenstates obtained from different boundary conditions which is achieved by diagonalizing block several times, each time with a different boundary condition. For detailed discussion see the paper of White and Noack (White and Noack, 1992). The Density Matrix Renormalization Group (DMRG) method proposed in the same paper is discussed in next chapter.

CHAPTER 2

Density Matrix Renormalization Group

In the previous chapter we saw why Wilson Numerical Renormalization failed to calculate the ground state energy properly. One of the solutions that was mentioned to rectify the error near the end of the last section does not work well for interacting system since the choice of boundary conditions that will give correct result is not clear. One thing that is clear from our earlier discussion is that to get the correct description of a block embedded in the environment it is necessary to connect and correlate it with the rest of the environment and any numerical procedure should just be able to do it. The DMRG method solves this problem by entangling the system block with the environment and then project out the most probable states of the block in the ground state by using reduced density matrix operator (White, 1992).

In what follows there will be a discussion of the Infinite and Finite DMRG algorithm and why density matrix leads to the optimal states in the system.

2.1 Infinite DMRG Algorithm

The main reason why we use Renormalization method is to keep Hilbert space from growing tremendously with system size. Suppose we have a spin=1/2 chain of length L in one dimension and we are interested in the ground state energy and various properties of ground state. L can be some finite number or thermodynamic limit $L \rightarrow \infty$. For the latter case we use Infinite DMRG algorithm in which the size of chain is increased by two sites at each step starting from $L = 2$. Here are the following steps.

Initially we start with two blocks A and B which in first step contains contains one site (spin) such that the no. of sites in the whole system is 2. Now we increase the size of left and right block (A and B) by introducing two spin in the middle of these two blocks such that the total length of chain becomes 4 and so on. With the addition of

two new spins in the middle the left and right block grown in size simultaneously by one site. If l is the current block size then after each step the size of block becomes $l + 1$ and the length of total chain becomes $L = 2l + 2$. Therefore the block state space grows exponentially as 2^l . In infinite DMRG algorithm at each step the chain has the following structure $A \bullet \bullet B$ where A is the system block, B is the environment block and together the whole structure is the universe or superblock.

In our case the local state space dimension i.e dimension of basis state of spin half denoted by d is 2. As the chain length increases the dimension of state space of system block A becomes 2^l where l is the size of block A after each iteration. Now in order to restrict the size of basis states of system block we need to restrict it to some given number m i.e we must effectively truncate the Hilbert space from some large number to a given m such that it still gives the exact estimate of the ground state energy and ground state wavefunction. Let us assume that the dimension of a system block A and environment block B is m . Then any superblock state at some particular instance $A \bullet \bullet B$ can be described by

$$|\psi\rangle = \sum_{i_A}^{m \times d} \sum_{i_B}^{m \times d} \psi_{i_A i_B} |i\rangle_A \otimes |j\rangle_B \quad (2.1)$$

$|i\rangle_A$ represents the tensor product of state space of system block A and one single site represented by the \bullet , hence the summation is upto the product of the dimension of these two state space $m \times d$ and similarly for $|j\rangle_B$. Therefore we see that after absorbing the single site the dimension of system block becomes md . The Hamiltonian of superblock which comprises of an enlarged system and environment block is constructed on the lines of step (4) given in the previous chapter. We will take up a particular example later. This Hamiltonian is diagonalised using Lanczos or Jacobi-Davidson method. Python uses Lanczos method and therefore in our program we have used Lanczos Algorithm. This gives us the ground state energy and corresponding eigenstate $|\psi\rangle$. In order to truncate the basis of system block to m we construct the reduced density operator for $A \bullet$ which is given by tracing out all the states of the environment block i.e $B \bullet$

$$\begin{aligned}
\hat{\rho}_{A\bullet} &= Tr_{B\bullet} \left(\sum_{i_A}^{m \times d} \sum_{j_B}^{m \times d} \sum_{i'_A}^{m \times d} \sum_{j'_B}^{m \times d} \psi_{i_A j_B} \psi_{i'_A j'_B}^* |i\rangle_A \otimes |j\rangle_B \otimes \langle j'|_B \otimes \langle i'|_A \right) \\
&= \langle j|_B \left(\sum_{i_A}^{m \times d} \sum_{j_B}^{m \times d} \sum_{i'_A}^{m \times d} \sum_{j'_B}^{m \times d} \psi_{i_A j_B} \psi_{i'_A j'_B}^* |i\rangle_A \otimes |j\rangle_B \otimes \langle j'|_B \otimes \langle i'|_A \right) |j\rangle_B \\
&= \sum_{i_A}^{m \times d} \sum_{j_B}^{m \times d} \sum_{i'_A}^{m \times d} \sum_{j'_B}^{m \times d} \psi_{i_A j_B} \psi_{i'_A j'_B}^* |i\rangle_A \otimes \langle j_B|j_B\rangle \otimes \langle j'_B|j_B\rangle \otimes \langle i'|_A \\
&= \sum_{i_A}^{m \times d} \sum_{j_B}^{m \times d} \sum_{i'_A}^{m \times d} \psi_{i_A j_B} \psi_{i'_A j_B}^* |i\rangle_A \otimes \langle i'|_A
\end{aligned} \tag{2.2}$$

Therefore this becomes

$$(\rho_{A\bullet})_{ii'} = \sum_{j_B}^{m \times d} \psi_{i_A j_B} \psi_{i'_A j_B}^* \tag{2.3}$$

This reduced density matrix considers the part $A\bullet$ as a system and $\bullet B$ as the statistical bath and is of the dimension $md \times md$. The eigenvalues and eigenstates of this density matrix is determined by diagonalisation and only certain number of states corresponding to the highest eigenvalues are kept and rest all are truncated (Schollwöck, 2011). This is the step that systematically leads to the truncation of Hilbert space. Instead of keeping all the md states of the enlarged block we only consider for example m states. This way number of basis state of our system block will never exceed m . These eigenstates with highest magnitude of eigenvalues correspond to the most probable states of the block $A\bullet$ in the ground state of the whole superblock. The sum of all the eigenvalues of the density matrix is equal to unity and therefore as a measure of truncation error we can find the quantity $\epsilon = 1 - \sum_{\alpha=1}^m w_\alpha$, where w_α is the eigenvalues of the density operator and the sum run to the m^{th} eigenvalue kept. This is the magnitude of the discarded eigenvalues and gives the indication of the accuracy of the system. In our calculation this quantity is usually of the order of 10^{-15} .

After finding these m states we form a rectangular matrix O where these m eigenstates of $\hat{\rho}$ are the column vector and the dimension of these O matrix are $md \times d$. This matrix is used to transform all operators defined on block $A\bullet$ into the new basis. This step is same as that of step (3) defined in the Wilson's RG method. Thus our new block

and all the operators are defined in this new basis which is of the dimension m . The corresponding procedure is applied to the environment block where all the operators defined on it are transformed into the reduced basis. The procedure is again repeated by introducing two new sites in between enlarged blocks and transforming the system until the desired length of the whole system is achieved. At each iteration the length becomes $2l + 2$ where l is the length of the system block and environment block which are increased equally in our algorithm. The Infinite DMRG algorithm can be stopped once the average ground state energy converges that is it reaches to a fixed value or the required accuracy (truncation error) is achieved.

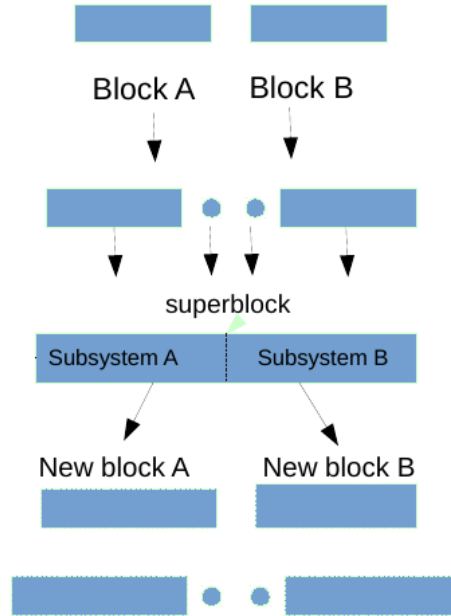


Figure 2.1: This figure shows the iterations taken in infinite system DMRG. New blocks are formed by integrating a site into a block. These blocks combine to form superblock and the new block has a truncated state space due to density matrix formulation. The growth happens on both the side leading to the chain growth (Schollwöck, 2011).

Initially we are interested in finding the ground state energy but for various lattice models we are required to calculate mass gap for which we need higher excited states. The states we are interested to find are called target states and we can't use the same expression of reduced density matrix that we found earlier since that was only targeted for ground state. In case when there are more than one target states the reduced density

matrix of the system block is defined as (Hallberg, 2006)

$$\rho_{ii'} = \sum_l p_l \sum_j \phi_{l,i_A j_B} \phi_{l,i'_A j_B} \quad (2.4)$$

where p_l defines the probability of finding the system in target state ϕ_l . In (2.3) l is 1 and p_l is 1 since our target state was only the ground state. This just shows that when the target state is other than ground state then the final density matrix of the system block is the combination of density matrix corresponding to all the target states weighed in according to their probability.

Now lets see how density matrix projection leads to optimal states in the system.

$$|\psi_0\rangle = \sum_{i_A}^M \sum_{i_B}^M \psi_{i_A j_B} |i\rangle_A \otimes |j\rangle_B \quad (2.5)$$

Let this be the state of the universe which consists of a system and the environment. Let M be the dimension of both the system and environment block. Now let us define another wave function $|\hat{\psi}_0\rangle$ defined in some reduced Hilbert space of dimension m . We would like to minimise the modulus of the difference of this wave function and true wave function i.e. $||\psi_0\rangle - |\hat{\psi}_0\rangle|^2$. This $|\hat{\psi}_0\rangle$ is given by

$$|\hat{\psi}_0\rangle = \sum_{\alpha_A}^m \sum_{j_B}^m a_{\alpha_A j_B} |\alpha\rangle_A \otimes |j\rangle_B \quad (2.6)$$

where $|\alpha\rangle_A = \sum_{i=1}^M U_{\alpha i_A} |i\rangle_A$ are the m system vector in an optimally reduced space which are linear combination of states of the system block of ψ . The square of the modulus of the difference of this new wave function and true wave function is the inner product of $||\psi_0\rangle - |\hat{\psi}_0\rangle|$ with its complex conjugate which is equal to

$$\begin{aligned} ||\psi_0\rangle - |\hat{\psi}_0\rangle|^2 &= \langle\psi_0|\psi_0\rangle - \langle\psi_0|\hat{\psi}_0\rangle - \langle\hat{\psi}_0|\psi_0\rangle + \langle\hat{\psi}_0|\hat{\psi}_0\rangle \\ &= 1 - 2 \sum_{\alpha j} \psi_{i_A j_B} a_{\alpha j} U_{\alpha i_A} + \sum_{\alpha j} a_{\alpha j}^2 \end{aligned} \quad (2.7)$$

where we have used the property $\langle\psi_0|\psi_0\rangle=1$ and for simplicity we have assumed that the coefficients of wave functions are all real which allow us to write $\langle\psi_0|\hat{\psi}_0\rangle = \langle\hat{\psi}_0|\psi_0\rangle$. Now to make (2.7) minimal we differentiate it with respect to $a_{\alpha j}$ and set the derivative

equal to zero, we get

$$\sum_i \psi_{ij} U_{\alpha i} = a_{\alpha j} \quad (2.8)$$

For notational convenience we have dropped label A and B as the subscript. Now if we substitute (2.8) back in (2.7) we get

$$1 - \sum_{\alpha i i' j} U_{\alpha i} \psi_{ij} \psi_{i'j} U_{\alpha i'} \quad (2.9)$$

In above equation we substitute our expression of reduced density matrix in (2.3) and then the equation becomes

$$1 - \sum_{\alpha i i'} U_{\alpha i} \rho_{ii'} U_{\alpha i'} = 1 - \sum_{\alpha}^m w_{\alpha} \quad (2.10)$$

$U_{\alpha i}$ are the coefficient that change the basis from system vectors $|i\rangle$ to $|\alpha\rangle$ and we identify w_{α} as the density matrix eigenvalues and $|\alpha\rangle$ as the corresponding eigenvectors (White, 1992). Compare this with (2.15). The above expression is minimum when using the largest m eigenvalues of ρ . Thus we can see the role of density matrix in giving the best approximation to the initial state by leading naturally to the best optimal reduced basis. (2.10) corresponds to the truncation error. For the connection of the above argument with Schmidt decomposition and Singular value decomposition (SVD) see section (2.3).

2.2 Finite DMRG Algorithm

After the desired length of our system is reached in infinite DMRG we usually follow it with finite DMRG algorithm to increase the accuracy of the ground state. The main difference from infinite DMRG is that here the length of the chain remains constant. Where in infinite DMRG the system block and environment block are both enlarged at the same time by introducing 2 sites in between, in finite DMRG one of the block is grown at the expense of other. Finite DMRG algorithm improve on the choice of reduced basis of the system state since now the superblock at any given instant has constant size unlike in infinite DMRG and the basis states of the system are determined with respect to it. Here is how the algorithm works

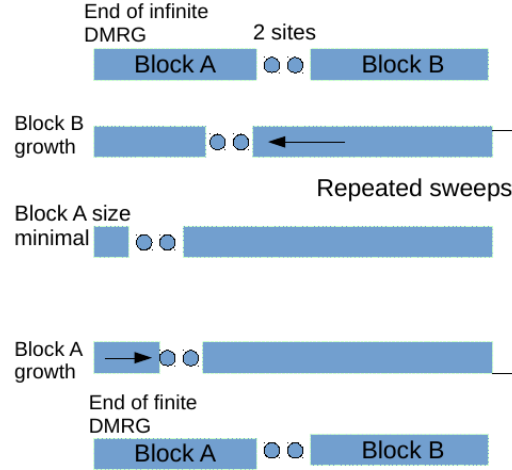


Figure 2.2: This figure shows the iterations taken in finite system DMRG. It starts from where Infinite DMRG ends. New blocks are formed by integrating a site into a block. These blocks combine to form superblock and the new block has a truncated state space due to density matrix formulation. Unlike Infinite DMRG growth happens only for one side at the expense of the other leading to constant chain length (Schollwöck, 2011).

At the end of infinite DMRG both the system and environment block is of equal size and we have the form $A \bullet \bullet B$. Now we grow block B at the expense of block A which shrinks using the infinite DMRG algorithm described previously which involves calculating the ground state of superblock formed from enlarged block B and shrunk block A , using that for reduced density operator, finding out its eigensystem and retaining the particular number of highest weight eigenvalues and eigenstates for the next iteration. This is carried out until block A is reduced to the minimum size i.e single site, after than the procedure is reversed and block A is grown at the expense of block B until it reduces to the minimum size. This one round of back and forth of growth direction ends when the size of both the blocks become equal and we get back the form $A \bullet \bullet B$. This is called one sweep. Based on the requirement that energy converges many number of sweeps may be required. In some calculation where number of reduced basis states kept is not the main criteria and we are only interested in finding the optimum solution to the lattice system we can perform each sweep with different number of reduced basis states to get more accurate solution. Of course for some lattice models energy converges to a fixed point easily without keeping too many reduced number of states.

Lets look at the algorithm in more detail. Suppose after an Infinite DMRG the chain length becomes L . Lets take $L = 30$. Then the system block and environment block

both have length $l = 15$. The information of system block and environment block after each iteration in infinite DMRG is stored. Now we want to increase the length of left block by a single site and decrease the length of right block at the same time by a single site. The new system and environment blocks are formed by enlarging the block of length 15 and 13 respectively whose information was already stored in the program. We follow the same procedure as we did before i.e. we enlarge these blocks by one site and form a superblock of system block of $l = 16$ and environment block of $l = 14$ and repeat the same steps as above. The information of the system and environment block is then updated. When I say information it means that at each step we account for the block length, basis states and operators defined on the block. Then again the system and environment blocks are formed by enlarging the block of length 16 and 12 and the superblock is formed with the system block of $l = 17$ and environment block of $l = 13$. This way we continue until we reached the system block of length 28. From there we increase the length of environment block at the expense of system block. Note that in finite DMRG the length of system block goes upto $L - 2$. Finite DMRG improves on the approximation of final system ground state taken during infinite DMRG .

2.3 Singular Value Decomposition and Schmidt Decomposition

The truncation procedure that is done in DMRG algorithm can be looked from the other perspective. We look at the Schmidt decomposition of our universe but before we do that we need to learn something about Singular Value Decomposition (SVD).

SVD takes an arbitrary matrix M of dimension $N_A \times N_B$ and decomposes it into

$$M = USV^\dagger \quad (2.11)$$

where U is of the dimension of $(N_A \times \min(N_A, N_B))$. The columns of U are orthogonal also called left singular vectors and therefore it has property $U^\dagger U = I$, if U is a square matrix i.e. $\min(N_A, N_B) = N_A$ then $UU^\dagger = I$ which implies it is Unitary. S is a square diagonal matrix of the dimension $\min(N_A, N_B) \times \min(N_A, N_B)$ with non

negative entries $S_{aa} = s_a$. These are called singular values. The schmidt rank of the matrix M is the number of non zero singular values in S . V^\dagger is of the dimension of $\min(N_A, N_B) \times N_B$ and has orthogonal rows (right singular vectors) and therefore $V^\dagger V = I$. If $\min(N_A, N_B) = N_B$ then it is Unitary with $VV^\dagger = I$.

Now let us apply the singular value decomposition to the state of the system $A \bullet \bullet B$. The state of the system as defined previously is given by

$$|\psi\rangle = \sum_{ij} \Psi_{ij} |i\rangle_A |j\rangle_B \quad (2.12)$$

where $|i\rangle_A$ and $|j\rangle_B$ are orthonormal bases of $A \bullet$ and $\bullet B$ with dimension $N_A = m \times d$ and $N_B = m \times d$. In our case block A and B have equal dimension but in general $N_A = N_B$ is not always true. The coefficient Ψ_{ij} is considered as a Ψ matrix now. In this representation reduced density operator $\hat{\rho}_A$ and $\hat{\rho}_B$ takes the matrix form and is given by

$$\rho_A = \Psi \Psi^\dagger \quad \rho_B = \Psi^\dagger \Psi \quad (2.13)$$

where we have dropped \bullet for notational convenience as we denote the enlarged system and environment block as A and B .

If an SVD is carried out on matrix Ψ of (2.12) we get

$$\begin{aligned} |\psi\rangle &= \sum_{ij} \sum_{a=1}^{\min(N_A, N_B)} U_{ia} S_{aa} V_{ja}^* |i\rangle_A |j\rangle_B \\ &= \sum_{a=1}^{\min(N_A, N_B)} \left(\sum_i U_{ia} |i\rangle_A \right) s_a \left(\sum_j V_{ja}^* |j\rangle_B \right) \\ &= \sum_{a=1}^{\min(N_A, N_B)} s_a |a\rangle_A |a\rangle_B \end{aligned} \quad (2.14)$$

The above form is called the spectral decomposition of the state. The ket vectors $|a\rangle_A$ and $|a\rangle_B$ are orthonormal because of the orthonormal properties of U and V^\dagger . If suppose now we restrict the sum to say any $m \leq \min(N_A, N_B)$ positive non zero singular values, we obtain the Schmidt decomposition. The state then becomes

$$|\psi\rangle = \sum_{a=1}^r s_a |a\rangle_A |a\rangle_B \quad (2.15)$$

If $r = 1$ we get a classical state where $|\psi\rangle$ is just simply the product of the kets $|a\rangle_A$ and $|a\rangle_B$. If $r > 1$ we have a entangled state since in that case $|\psi\rangle$ cannot be written as a product of two separate kets. In this representation it is easy to see that reduced density operators are given by

$$\hat{\rho}_A = \sum_{a=1}^r s_a^2 |a\rangle_A \langle a| \quad \hat{\rho}_B = \sum_{a=1}^r s_a^2 |a\rangle_B \langle a| \quad (2.16)$$

The $w_a = s_a^2$ are the eigenvalues of the both reduced density matrix operator and it is the square of the singular values. The Von Neumann entanglement entropy is given by

$$S_{A|B} = -\text{Tr} \hat{\rho}_A \log_2 \hat{\rho}_A = -\sum_{a=1}^r s_a^2 \log_2 s_a^2 \quad (2.17)$$

The truncation of Hilbert space can be done using SVD where the new state $|\tilde{\psi}\rangle$ spans over state spaces of A and B which have dimension $r' < r$. The 2-norm of $|\psi\rangle$ is equal to the Frobenius norm of the matrix if $|i\rangle$ and $|j\rangle$ are orthonormal therefore

$$||\psi\rangle||_2^2 = \sum_{ij} |\psi_{ij}|^2 = ||\psi||_F^2 \quad (2.18)$$

Therefore for optical approximation of the 2-norm of the matrix $|\psi\rangle$ with $|\tilde{\psi}\rangle$ one can instead use Frobenius norm of ψ by $\tilde{\psi}$ where the latter is a matrix rank of r' . Following (2.14) we can write $\psi = USV^\dagger$ with $S = \text{diag}(s_1, s_2, \dots, s_r)$ where the rank of ψ is r . The new state $\tilde{\psi}$ can be decomposed as $\tilde{\psi} = US'V^\dagger$ where $S' = \text{diag}(s_1, s_2, \dots, s_{r'}, 0, \dots)$. This S' is constructed from r' largest singular values of ψ and setting all other equal to zero. The column dimension of U and V^\dagger will shrink accordingly. This discussion has already been carried out in the previous section but here we see this with different perspective. The Schmidt decomposition of the approximate state is given as

$$|\tilde{\psi}\rangle = \sum_{a=1}^{r'} s_a |a\rangle_A |a\rangle_B \quad (2.19)$$

2.4 Why DMRG works?

While examining the eigenvalues of the reduced density matrix of the system $|\psi\rangle$ we can easily figure out how effective DMRG approximation has been. Its efficiency sim-

ply depends on how quickly the eigenvalues w_a decreases. It has been found that in one dimension for gapped system eigenvalues decay exponentially fast (roughly as $e^{-c \ln^2 a}$) and therefore the truncation error which is nothing but the sum of discarded eigenvalues is very small since these eigenvalues does not contribute much to the system. Hence DMRG works very well in one dimension. In two dimension for width W , $c \propto 1/W$ such that increasing the width W of the lattice system will cause the eigenspectrum to decay so slow and therefore the truncation error will increase making DMRG inefficient.

Another way to look at this is to consider entanglement entropy. We use something called Area law for entanglement entropy which says that for ground state of short ranged gapped Hamiltonian entanglement entropy is not extensive but is proportional to the surface. If $A|B$ is a bipartition and A is of size $L^{\mathcal{D}}$, with \mathcal{D} is the spatial dimension then in the thermodynamic limit $S(A|B) \propto L^{\mathcal{D}-1}$ as opposed to thermal entropy. Therefore in one dimension $S \propto \text{constant}$ and $S \propto L$ in two dimension. Near criticality we see that $S \propto \frac{c}{6} \log_2 L + k$ where c is the central charge that comes from conformal field theory, whereas fermionic system in two dimension goes like $S \propto L \log_2 L$.

The entanglement entropy between system A and B is given by $S = \log_2 D$ where D is the dimension of state space. From the above argument it is clear that for gapped system in one dimension $D \propto 2^k$ where k is some constant and hence increasing the system size will not lead to increase in D . However in 2 dimension $D \propto 2^L$ such that DMRG will fail even for relatively small sizes as resources will have to grow exponentially. Similarly near the critical region of one dimension $D \propto L^{\frac{c}{6}}$ which means that the growth of D is sufficiently slow (since power is usually $1/3$ or $1/6$) such that large system size can be reached.

2.5 Measurement of Observables and Ground state properties

We have already seen how to calculate the entanglement entropy between the system block and the environment block. It is given by (2.17) where we use the eigenvalues of reduced density matrix for system block. At each iteration of the finite system algorithm we can calculate the entanglement entropy and get the corresponding Von Neumann

entropy for different size of system block. Using this we can study the form of the relation between size of the system block and entanglement entropy and compare it with the theoretical expression.

The other important property that we can calculate for the lattice models is the mass gap. Mass gap is the difference between the ground state energy and the first excited state energy. It is a very good indication of phase transition wherein the mass gap may vanish in one phase but remain non zero in other. More on the importance of mass gap will be seen when the mass gap for the Transverse Ising model is calculated. To calculate mass gap one need to have more than one target state in the DMRG algorithm. Since the state vector in the ground state may contribute to the first excited state as well as there may be some contribution from the higher excited energy state vectors, the resultant density matrix should be the combination of various energy state vectors as given in (2.4).

In the finite system algorithm the ground state energy is minimum when the system and environment block is of the same size within the superblock. This is called the symmetric configuration and all other observables such as one and two point correlation function and order parameter are measured with respect to this symmetric state. The expectation value or one point correlation function of S_i^z at site i is given by

$$\langle S_i^z \rangle = \langle \psi_0 | S_i^z | \psi_0 \rangle \quad (2.20)$$

where ψ_0 is the ground state. The problem associated with the above formula during the implementation is that after each iteration the ground state changes because of the change in the basis and therefore one cannot know beforehand the final state. Suppose we add a spin at site i and we want to know the expectation value of S^z on this site. The representation of S_z operator in the basis of enlarged block at site i is given by

$$I_b \otimes S_d^z \quad (2.21)$$

where I_b is the Identity matrix of block before adding the i_{th} site. The dimension of this matrix is some $m \times m$ which is the dimension of block basis states in a truncated Hilbert space from previous iteration. The operator S^z added on the site i has dimension d which in our case for spin half particle is 2. After adding this site this operator in enlarged block basis states undergoes basis transformation and is truncated to the m

basis states. In general we can calculate the expectation value now but since the symmetric state is not reached yet this will give error. Therefore in order for this operator which we denote by S_i^z to have right representation when the symmetric configuration is reached, it is updated and modified every time the basis change and we get it in new truncated basis by performing transformation using matrix O and O^\dagger as mentioned in the DMRG algorithm.

Let us look at how the operator is updated in more detail. (2.21) gives us the representation of S_z at site i in the basis of enlarged block with i sites before truncation. Let us denote it by $(S_i^z)^e$ then the representation of S^z at site i after truncation is given by

$$(S_i^z)_i = O_i (S_i^z)^e O_i^\dagger \quad (2.22)$$

After this we add another site at $i + 1$, the representation of S^z at site i in this enlarged block basis is given by

$$(S_i^z)_{i+1}^e = (S_i^z)_i \otimes I_d \quad (2.23)$$

where the form of the above equation is similar to (2.21) except it is computed at $(i+1)^{th}$ site. The superscript e denotes that it hasn't been truncated yet and it is the representation in the enlarged block. It is then truncated with O_{i+1} . This ensures that we always have representation of the operator in the current basis. This process is carried out till we reach the symmetric state where system and environment block is equal to each other. Note that upto now we have the representation of the operator whose expectation value we need in the system block. Now in order to carry out the operation of (2.20) we need the representation of this operator in the Hilbert space of the superblock. This is done by taking the tensor product of the representation of S^z in the final system block with the Identity operator corresponding to the two sites in the middle and Identity operator acting on the environment block. The dimension of the Identity operator acting on the environment block is of the dimension of the truncated Hilbert space i.e. $m \times m$. What's left is the final $|\psi_0\rangle$ in this symmetric state on which this operator is acted upon which we have an easy access during finite system algorithm. In order to get more accurate results it is best not to calculate one point correlation function on a site i which is near the far end from the middle of the block. As we know that after each site is added we have to perform a truncation on our observable and therefore if the site is very close to the beginning that means the operator will undergo lot of basis transformation and

that reduces the accuracy. Therefore a greater accuracy is achieved from the observable that are near the middle of the chain.

After being able to deal with one point correlation function we discuss non local operators like two point correlation function denoted by $C_s(i, j) = \langle S_i^z S_j^z \rangle$. Well one way to do that is take the representation of operator S^z at site i and j by the procedure described in the previous paragraph and simply multiply them and get the $C_s(i, j)$. Lets look at an example of spin-spin correlation at $j = i + 1$ where we calculate two point spin correlation between neighbouring sites and for notational convenience the symmetric configuration is reached at $i + 2$. The representation of operator S_i^z and S_j^z in the symmetric state of the chain size of $i + 2$ is given by

$$\begin{aligned} (S_i^z)_{i+2}^e &= (O_{i+1}((O_i(I_b \otimes S^z)O_i^\dagger) \otimes I_d)O_{i+1}^\dagger \otimes I_d \\ (S_{i+1}^z)_{i+2}^e &= (O_{i+1}(I_b \otimes S^z)O_{i+1}^\dagger) \otimes I_d \end{aligned} \quad (2.24)$$

Note that we haven't yet truncated the representation of these two operators on site $i + 2$. Multiplying these two for spin correlation function we get

$$(S_i^z S_{i+1}^z)_{i+2}^e = (O_{i+1}((O_i(I_b \otimes S^z)O_i^\dagger) \otimes I_d)O_{i+1}^\dagger (O_{i+1}(I_b \otimes S^z)O_{i+1}^\dagger) \otimes I_d \quad (2.25)$$

We can calculate this with the other way which seem much more effective in terms of accuracy that is we multiply the two operators as soon as the j^{th} site is added and not wait for the system to reach $i + 2$ site as we did in the (2.24). This gives us

$$C_s(i, i + 1)_{i+1} = O_{i+1}(((O_i(I_b \otimes S^z)O_i^\dagger) \otimes I_d)(I_b \otimes S^z))O_{i+1}^\dagger \quad (2.26)$$

The two O_{i+1} and O_{i+1}^\dagger at the beginning and end transform the basis to reduced Hilbert space of the enlarged block with $i+1$ sites. From this step onwards $(C_s(i, i + 1))_{i+1}$ is transformed as whole like our (S_i^z) in the previous discussions. Its representation in the enlarged block at $i+2$ site is given by

$$(C_s(i, i + 1))_{i+2}^e = C_s(i, i + 1)_{i+1} \otimes I_d \quad (2.27)$$

If we compare (2.25) and ((2.27) we can see that only a factor of $O_{i+1}^\dagger O_{i+1}$ is missing from (2.27). If there was no truncation of state then this product would be a unity and both the equation would be same but with truncation this is not true and the factor

$O_{i+1}^\dagger O_{i+1}$ leads to the loss of accuracy in matrix multiplication. If the sites i and j are far away then the error becomes more because of the many pair of $O^\dagger O$ that gets added with each separating site between i and j . Therefore in our algorithm we use the second method and multiply the operators as soon as possible and store it and update it each time we change the basis.

CHAPTER 3

Transverse Ising Model

The Hamiltonian for Transverse Ising Model(TIM) is given by

$$H = - \sum_{\langle ij \rangle} J \hat{S}_i^z \hat{S}_{i+1}^z - h_x \sum_i \hat{S}_i^x \quad (3.1)$$

This Hamiltonian represents the interaction between nearest neighbour which we denote by $\langle ij \rangle$. The negative sign ensures that the energy is minimum (Ground State) when all the spins are aligned in one direction either up or down. The second term indicates that the external magnetic field is applied in \hat{x} -direction. The \hat{S}^i are the usual spin 1/2 Pauli operators given by

$$\hat{S}^x = \begin{pmatrix} 0 & 1 \\ 1 & 0 \end{pmatrix}, \hat{S}^y = \begin{pmatrix} 0 & -i \\ i & 0 \end{pmatrix}, \hat{S}^z = \begin{pmatrix} 1 & 0 \\ 0 & -1 \end{pmatrix} \quad (3.2)$$

3.1 Formation of superblock in Transverse Ising Model

Before we proceed to give the numerical results based on DMRG for the TIM lets address how DMRG will work for the above model and how we will go about forming the Hamiltonian of the superblock and connection operator defined on the system and environment block in our algorithm and its truncation and transformation to the new basis. We will illustrate the full DMRG step of enlargement and truncation for the TIM model.

We will start with a initial system block which has only a single site. The identical block is considered for the initial environment block. The single site Hamiltonian defined on the initial system and environment block will be just $H_{BS} = H_{BE} = -\hat{S}^x$ since it consist of only one site. The subscript BS and BE is to distinguish between system and environment block. The connection operator defined on this block which is used to connect to the neighbouring site is \hat{S}_b^z . We have taken h_x and J equal to one for the present discussion. Now the DMRG step for enlarging the block is done by introducing

two new sites between the initial system and environment block and enlarging each block with one site. We are working in \hat{S}^z basis. The Hamiltonian of the enlarged block is given by

$$\begin{aligned} H_{eS} &= H_{BS} \otimes I_d - I_B \otimes H_B - \hat{S}_{BS}^z \otimes \hat{S}_d^z \\ H_{eE} &= I_d \otimes H_{BE} - H_{BE} \otimes I_B - \hat{S}_d^z \otimes \hat{S}_{BE}^z \end{aligned} \quad (3.3)$$

where H_{eS} and H_{eE} are the Hamiltonian of enlarged system and environment block. We see that the site is added on the right side of the system block and left side of the environment block. I_d is the unit operator acting on a single site which is of dimension 2 (spin 1/2). \hat{S}_d^z is the \hat{S}^z operator on the single site and \hat{S}_{BS}^z and \hat{S}_{BE}^z are the representation of \hat{S}^z in the basis of the system and environment block. This is equal to \hat{S}_d^z for just an initial block with one site. I_B is the unit operator on the block which is same for system and environment block. In addition to the Hamiltonian of the enlarged block one also need the representation of the connection operator which are the spin operators of the newly added rightmost site (leftmost site) to the system (environment) block in the enlarged block basis. In order to construct the representation of these connection operator in the basis of enlarged block we have to construct the tensor product of the unit matrix on the block Hilbert space and the operator on the Hilbert basis of the rightmost site. In TIM this operator is \hat{S}_d^z . The representation of this operator in the enlarged block basis $(\hat{S}_r^z)_e$ is given by

$$\begin{aligned} (\hat{S}_r^z)_{eS} &= I_B \otimes \hat{S}_d^z \\ (\hat{S}_l^z)_{eE} &= \hat{S}_d^z \otimes I_B \end{aligned} \quad (3.4)$$

where r and l denotes right and left side. Just like with our enlarged Hamiltonian block, our connection operator for enlarged system and environment block will have different form and order. The superblock in Infinite DMRG is then constructed by taking the enlarged system block as the left block and connecting it to the enlarged environment block on the right. This connection is done by connection operator whose representation is given in (3.4). The Hamiltonian of the superblock is given by

$$H_s = H_{eS} \otimes I_{eE} + I_{eS} \otimes H_{eE} - (\hat{S}_r^z)_{eS} \otimes (\hat{S}_l^z)_{eE} \quad (3.5)$$

I_{eE} and I_{eS} are the unit operator on the Hilbert space of the enlarged block which is of the dimension 2^l where l is the number of sites in the enlarged block. The dimension for unit operator on the enlarged block is then 4×4 . Similarly dimension of the connection operator is 4×4 . The dimension of our superblock is then given by 16×16 . We then diagonalise this superblock to get ground state energy and corresponding eigenvector $|\psi_0\rangle$. The dimension of $|\psi_0\rangle$ is 16×1 . This is then recasted in the form of 4×4 matrix. From this we find reduced density matrix (see (2.13)). The transformation matrix O is then formed from the largest eigenvectors of this reduced density matrix. In the initial stages there is no truncation since the Hilbert space is small and therefore O and O^\dagger are of the dimension 4×4 . After constructing these transformation matrix we apply it on the connection operator in (3.2) and Hamiltonian of enlarged block in (3.3) as shown in (2.23) to get representation of these operators in this new transformed basis. After truncation we relabel H_{eS} , H_{eE} as H_{BS} , H_{BE} and $(\hat{S}_r^z)_{eS}$, $(\hat{S}_l^z)_{eE}$ as \hat{S}_{BS}^z and \hat{S}_{BE}^z . The whole process is then repeated from (3.3). Note that once the Hilbert space dimension grows up to some given m so that truncation comes into the picture the dimension of H_{BS} and other operators defined on the block after truncation have matrices of dimension $m \times m$.

3.2 Numerical Results

Now that we have got the formation of superblock and the connection operator out of the way we can proceed to give the numerical results computed on TIM with our DMRG method. Rewriting the (3.1) as

$$H = -J \left[\sum_{\langle ij \rangle} \hat{S}_i^z \hat{S}_{i+1}^z - \frac{h_x}{J} \sum_i \hat{S}_i^x \right] \quad (3.6)$$

The Hamiltonian is scaled with coupling constant $J = 1$. The spin operators satisfy usual commutation relations. For a system like this we can, from duality symmetry show that there exists a critical point and it is equal to $\frac{h_x}{J} = 1$ that is $J = h_x = 1$ (Sei Suzuki and Chakrabarti, 2013). Setting $J = 1$ the high field ($h_x > 1$) is a paramagnetic phase and the low field ($h_x < 1$) is a ferromagnetic phase. Therefore $\frac{h_x}{J} = 1$ is a critical point and we observe a quantum phase transition. Besides finding

the ground state energy for such models DMRG very effectively looks for the signature of phase transition and predicts the behaviour of the system as the parameter is changed. At the critical point the ground state energy for a finite system with open boundary conditions is given by:

$$E/J = 1 - \operatorname{cosec}\left(\frac{\pi}{2(2L+1)}\right) \quad (3.7)$$

So to get the ball rolling first we look at how the energy behaves at critical point with the system size in Infinite algorithm. The Hilbert space is truncated at $m = 30$ basis states. To see how the number of reduced basis states kept affect the relative accuracy, in Figure

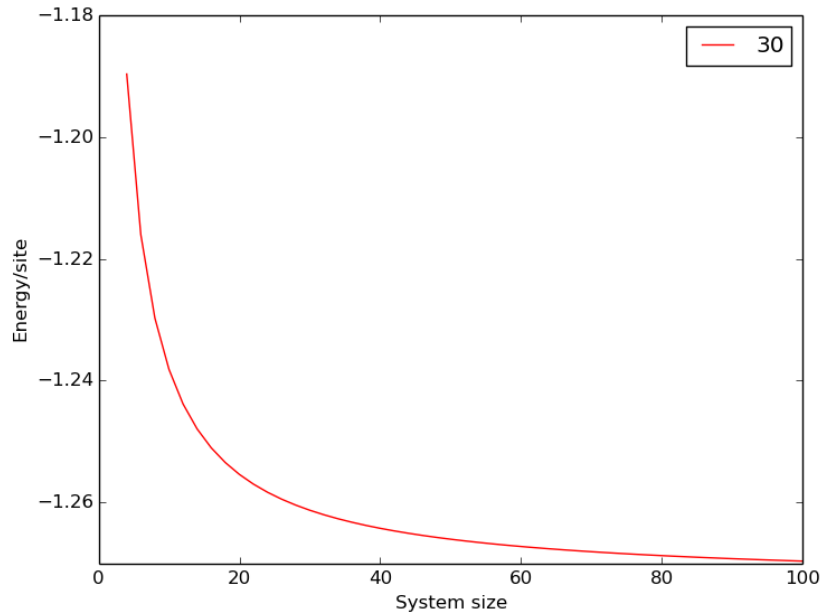


Figure 3.1: Plot of Energy dependence on the system size calculated with Infinite DMRG upto 100 sites with $m = 30$. We can see that energy falls very sharply at the initial sizes but then attain a slow gradual decline

3.2 we have calculated ground state energy at each step of infinite DMRG with different number of basis states like 5,10,20,30 and 40 and then plotted their energy difference to see how they change with the system size. The dashed line and horizontal dashed line is the difference in the ground state energy for 5 and 30 basis states kept and 5 and 40 basis states kept respectively. As one can probably guess for this scenario the energy difference increases with the system size since the ground state energy found by using 5 basis states will be fine upto small number of sites as seen in the figure but as the system size increases it will give highly incorrect estimate of ground state energy because of

the large truncation error associated with such small number of reduced basis states and will deviate from the estimates given by the the infinite DMRG using higher basis states. Next in the figure the solid line and circles represents the difference in the ground state energy of Infinite DMRG with 20 and 40 basis kept and 20 and 30 basis kept. We see that as the system size increases to 50 sites the difference is constant and almost zero so this tells us that we can use either of these three dimension of reduced basis states for our calculations and our ground state energy will be more or less same. Next we use

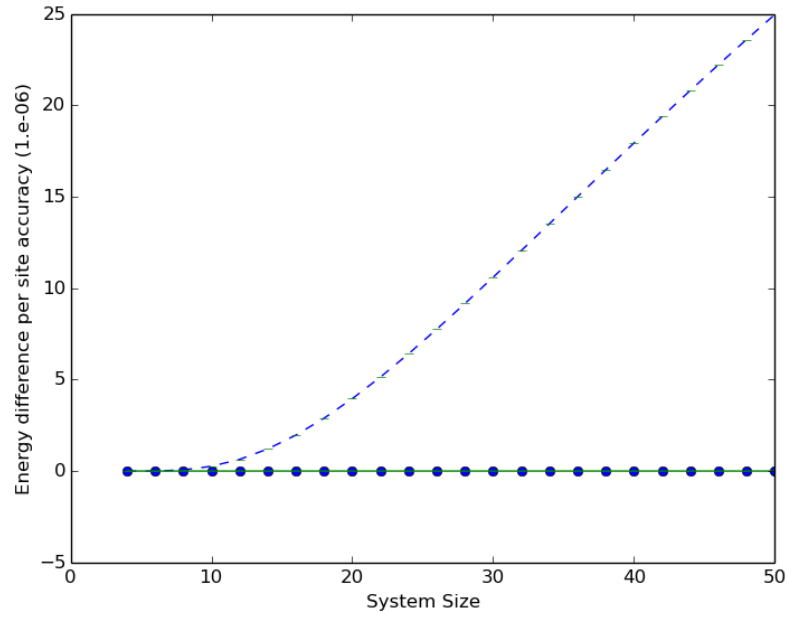


Figure 3.2: Plot of energy difference of ground state vs the system size for various number of basis states kept in infinite DMRG. The dashed line and horizontal dashed line is the difference in the ground state energy for 5 and 30 basis states kept and 5 and 40 basis states kept respectively, the solid line and circles represents the difference in the ground state energy of Infinite DMRG with 20 and 40 basis kept and 20 and 30 basis kept. Total number of sites are 50.

finite DMRG method to see how the energy converges at critical point to some value for TIM. We ran the finite DMRG algorithm keeping the dimension of reduced Hilbert basis states to 30. The ground state energy converges to a fixed value in just one whole sweep after undergoing the elongation of left block and right block. This is usually not true for other complicated interacting system which require repeated sweeps to undergo the convergence and which may give the illusion of convergence in initial sweeps but than the value of energy starts to change so just to be sure we did repeated sweeps each time with different basis states and there was no fluctuation in the ground state energy

and it was convergent at the same value. Figure 3.3 shows one such sweep in the finite DMRG method for $L = 20$ sites. Iteration is defined as one single dmrg step where a site is added and the ground state of superblock is found. The first iteration is when the system block at left side becomes of size 10 and at 8^{th} iteration after it has reached $L - 2$ the right side block starts to increase in size from 2 and at 16^{th} iteration it again reaches to the centre of block and keep growing towards left. The energy changes till

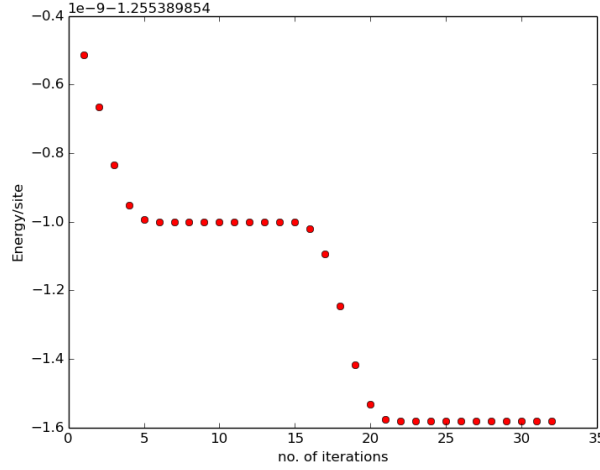


Figure 3.3: This plot shows how energy changes with each step of finite DMRG. No of site is 20 and we start from the middle of the block. For few steps energy is changing before taking on a constant value for left block. The right block then starts growing having the same constant energy when it reaches in middle and from there energy starts to decrease again till it reaches the final converged value at 20th iteration after which it does not change in later sweeps.

20th iteration and after that there is no change and the last iteration is when both blocks are of equal size with two sites in between. This is called one sweep.

The energy reaches to a fixed point after one sweep. The numerical results of ground state energy for 16, 20, 40 sites are -1.2510, -1.2554, -1.2642. The ground state energy for 20 sites can also be read off from the figure. These results match perfectly with the exact results that we get after putting various system sizes in (3.7).

Next we look at the behaviour of entanglement entropy for TIM. Entanglement entropy is not only important in Quantum information but it has also found appreciation in condensed matter theory with its behavior near the critical point. The idea that there is a relationship between entanglement entropy and Quantum phase transition is been taken seriously since entanglement is a measure of quantum correlation that drive the system across phase transition. In one dimensional magnetic systems entanglement

shows scaling behaviour in the vicinity of the transition point. We have calculated the bipartite (Von Neumann) entanglement entropy at the center of the chain between two blocks during the infinite system algorithm and showed its dependence on the size of the system in Figure 3.4. We can see that the dependence is same for two different dimension of reduced Hilbert space reasserting our previous results that any of those two can be used for our calculations.

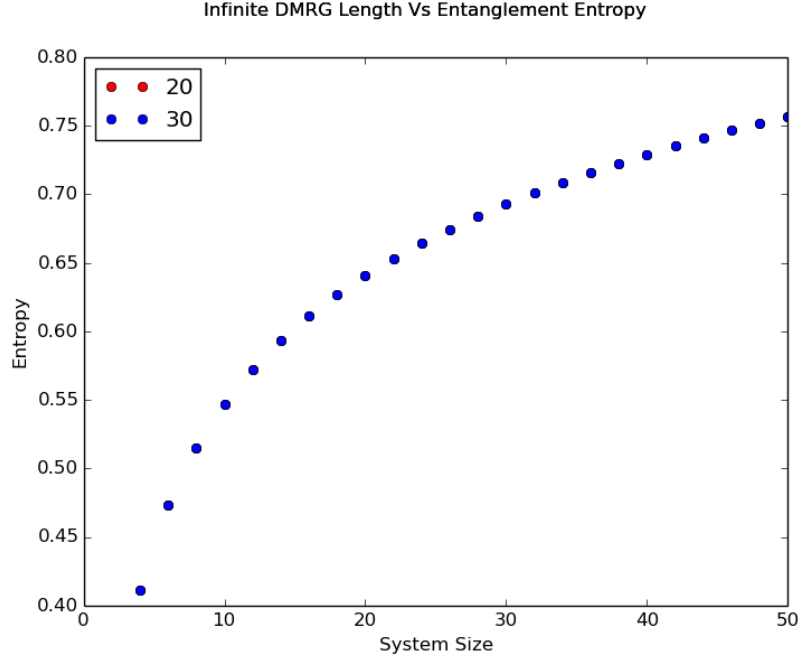


Figure 3.4: Entanglement Entropy Vs the system size during each step of Infinte DMRG upto 50 sites.

Next we look at bipartite entanglement entropy for every bipartite splitting. That is we have plotted the entanglement entropy between block A and block B for each size of block A in finite size DMRG with total system size of 50 , 100 and 200 sites for $m = 30$. It can be seen that the entropy is maximum at the centre of the chain when the size of both block A and block B is equal. From this figure we can calculate the central charge c for the one dimensional Ising model. The entanglement entropy of a central charge c on a system with open boundary conditions is

$$S = \frac{c}{6} \left[\log_2 \left[\frac{L}{\pi} \sin \frac{\pi x}{L} \right] \right] + k \quad (3.8)$$

where x is the subsystem size and L is the total length of the system. We fit the plot in Figure 3.5 with the function $y = A \log_2 x + k$. For 50 sites we found A and k to be 0.08889 and 0.40285 respectively. Using this we can calculate central charge of the

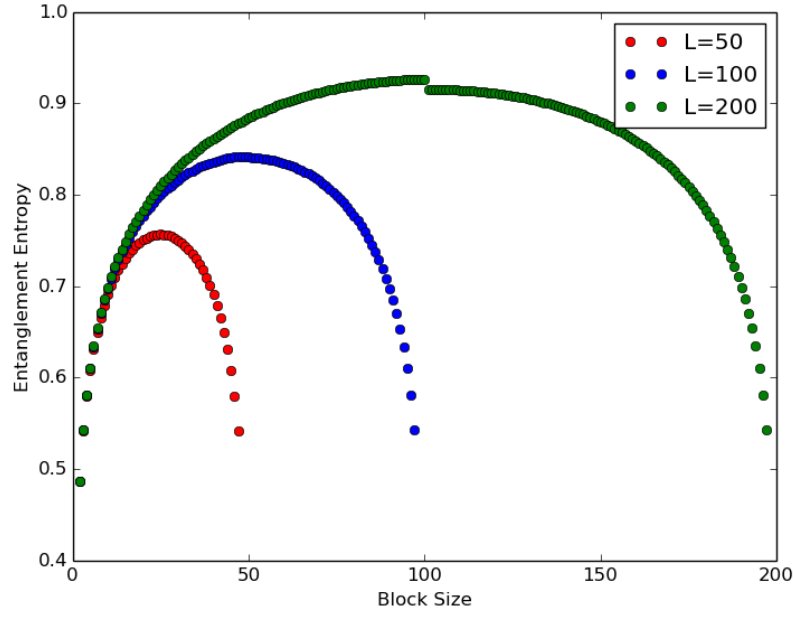


Figure 3.5: Entanglement Entropy of the subsystem of different sizes using finite DMRG within the total length of 50,100 and 200 sites keeping $m=30$.

system which comes out to be $c = 0.53334$. Similarly using the above procedure we find that for sites 100 and 200 the central charge respectively is 0.5216 and 0.5060 with the average being 0.5203 which is close to the theoretical value of $c = 0.5$

After looking at the energy and entanglement entropy at the critical point now we look at the variation in the ground state energy with respect to the parameter hx/J which is varied by changing the magnetic field. The ground state energy decreases monotonically with transverse field and is non analytic around $hx/J = 1$ which is the point where quantum phase transition happens.

The Hamiltonian governing the microscopic behaviour of quantum system results in different macroscopic configuration which we like to say as 'phase'. The transition between such phases can be observed by looking at order parameter which has a non zero value in one phase while null in other phase. In Figure 3.7 we have plotted the transverse order parameter $\langle S_x \rangle$ and longitudinal order parameter $\langle S_z \rangle$ with respect to the external transverse magnetic field. It is seen that $\langle S_x \rangle$ has nice form and is non analytic near the critical point but $\langle S_z \rangle$ value is not in a definite pattern as it should be since the low field phase is a ferromagnet phase. This is because the Hamiltonian has an up-down symmetry which is the reason why $\langle S_z \rangle$ is not properly defined.

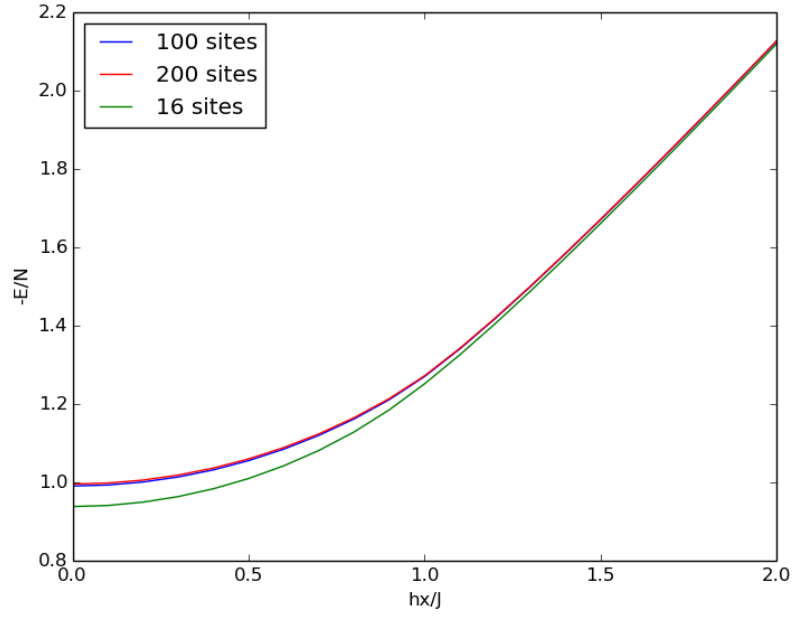


Figure 3.6: Ground state energy vs h_x/J for 50, 100 and 200 sites keeping $m=30$.

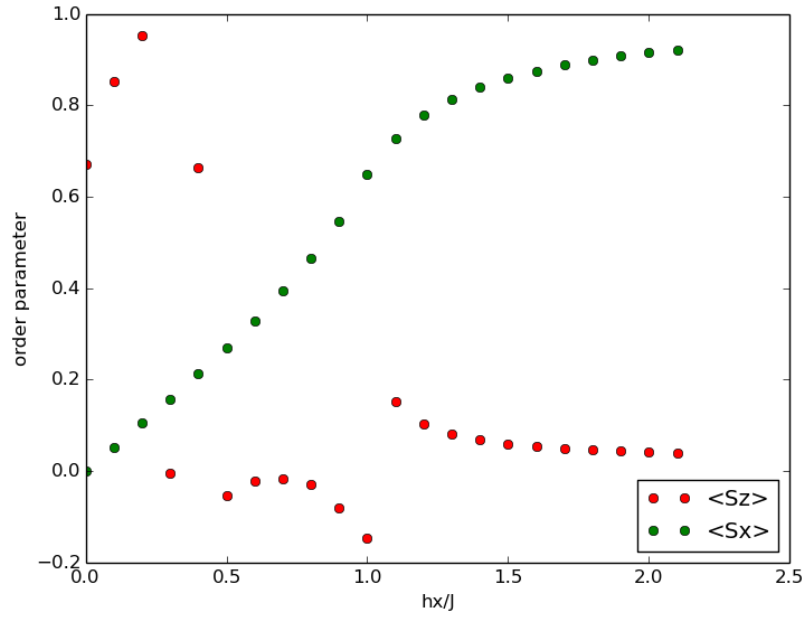


Figure 3.7: Order parameter variation with transverse magnetic field for 50 sites without any bias

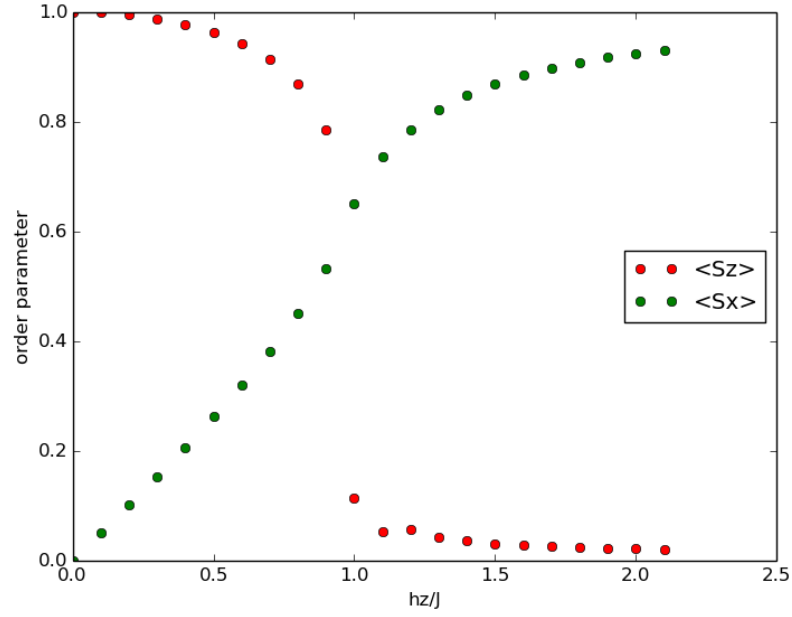


Figure 3.8: Order parameter for 100 sites with respect to transverse magnetic field for $m=30$ with an external bias magnetic field in longitudinal direction applied to the Hamiltonian.

The longitudinal order parameter cannot be evaluated directly unless we break this symmetry by applying a small bias field in the longitudinal direction. Therefore we add a term $-h_z \sum_i \hat{S}_i^z$ to the Hamiltonian where $h_z = 0.0002$. The effect can be seen in Figure 3.8 where now $\langle S_z \rangle$ can be seen to have change its form at $h_x = 1$ near the critical point where it goes from ferromagnetic phase (all spin up or all spin down) to a paramagnetic phase with longitudinal order parameter going to zero. The same argument goes for transverse order parameter and together their curve have kink and anti-kink form.

The best measure of phase transition in Transverse Ising model is perhaps given by mass gap which is the difference between the first excited state and the ground state. For quantum phase transition the inverse of mass gap of Hamiltonian gives the correlation length, so near the critical point when correlation length tends to infinity, mass gap goes to zero. In Figure 3.9 we can see how the mass gap for various system size behaves when the magnetic field h_x changes. We can see that as the size of the system increases the vanishing point for mass gap approaches towards the point $h_x = 1$ which one can estimate as being the critical point in the thermodynamic limit.

Now we will look at variation of entanglement with respect to J/h_x where we scale our Hamiltonian with magnetic field and set it equal to $h_x = 1$ earlier we set $J = 1$. In

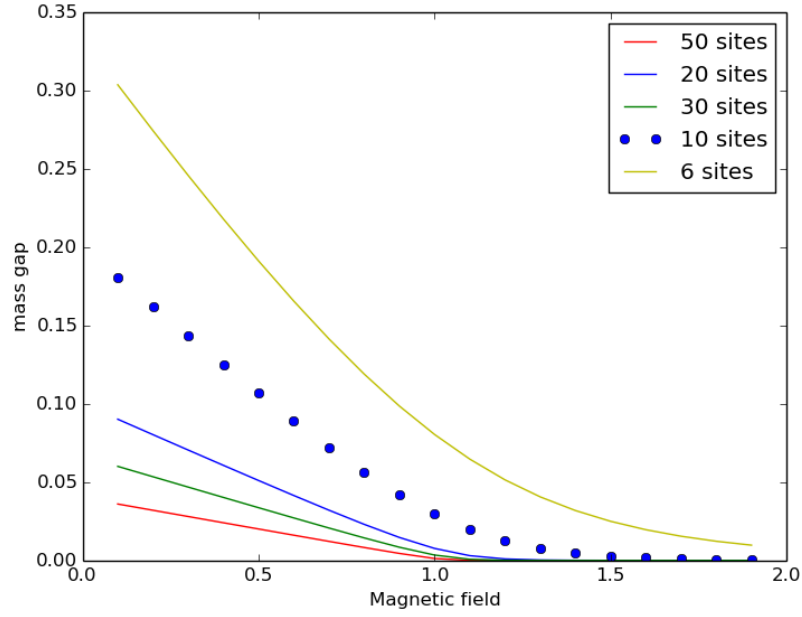
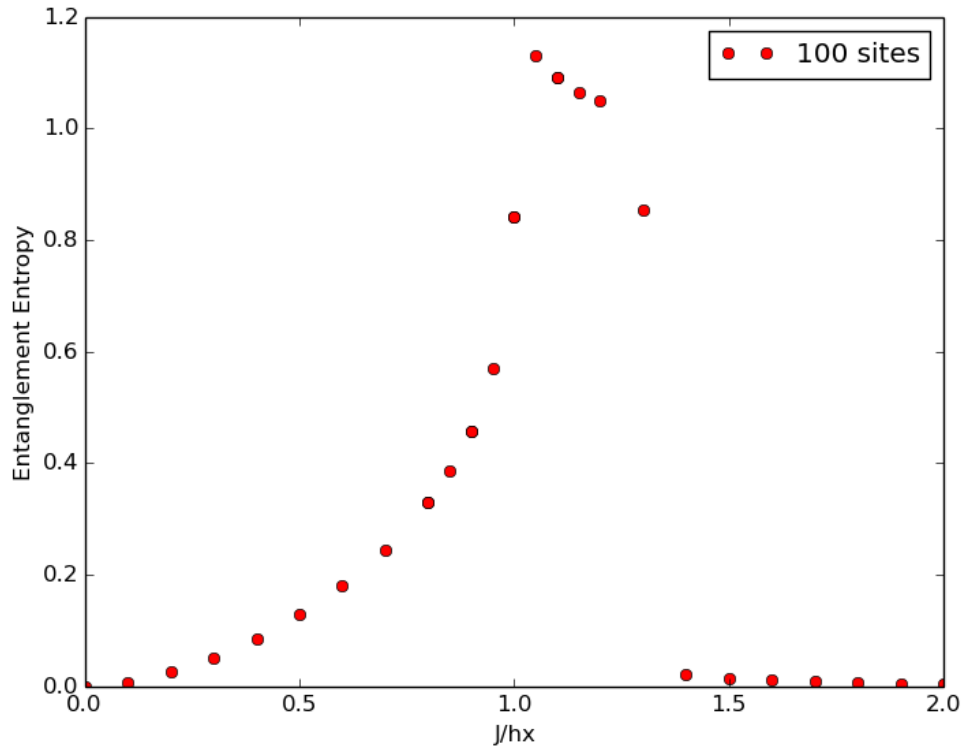


Figure 3.9: Mass gap variation with J/h_x for various system sizes. For $J/h_x < 1$ is a paramagnet phase and near the phase transition mass gap goes to zero and system becomes gapless.

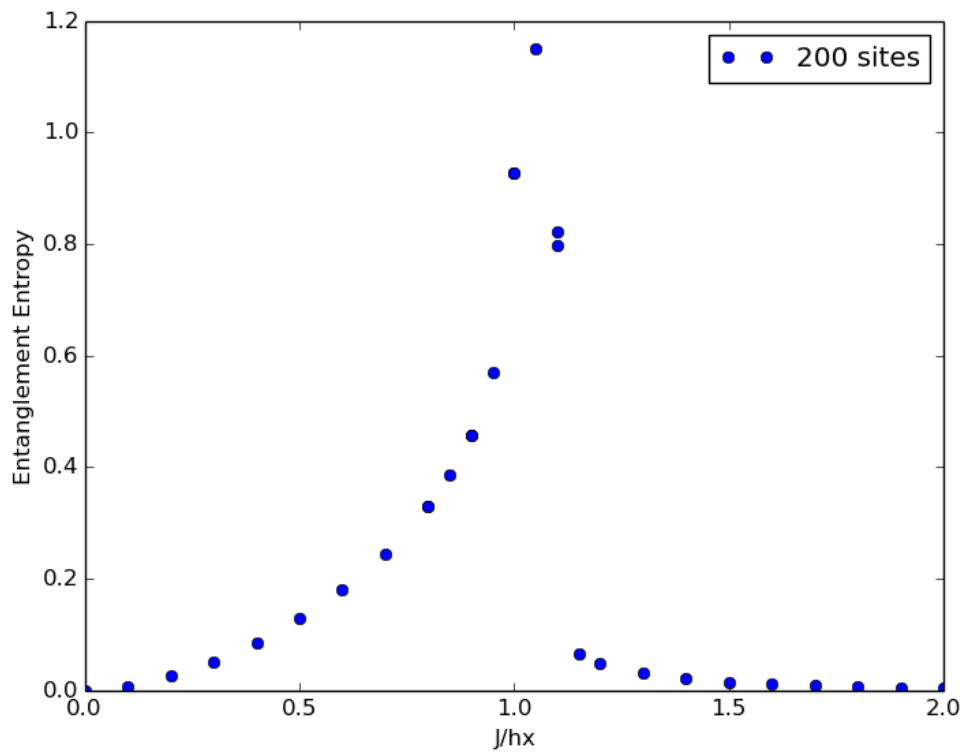
general entanglement increases when the system approaches the quantum phase transition. The measure of the entanglement is entanglement entropy between two blocks A and B . Entanglement entropy vanishes if the subsystem A decouples from subsystem B .

As seen in the Figure 3.5 the entanglement entropy is maximum at the centre of the chain therefore we have studied the variation of entanglement entropy in Figure 3.10a and 3.10b at the centre of the chain with respect to the change in J/h_x . It can be seen that at the critical point the entanglement entropy is maximum and for Figure 3.10b the change is sharp near the critical point in comparison to the Figure 3.10a. Theoretically when the system size reaches infinity the entropy encounters singularity at $h_x = J = 1$ and it becomes proportional to $\log_2 2$ when $h_x = 0$ since the ground state is doubly degenerate for the ferromagnetic phase $J/h_x > 1$. Therefore we expect better results towards the end of the graph and sharp transition near the critical point if no. of sites are increased to a very large number. But one thing that is clear from the graphs are that it show the presence of quantum phase transition. Similar to this is Rényi entropy given by

$$S_k(\rho) = \log_2 \frac{\text{Tr}(\hat{\rho}^k)}{1 - k} \quad (3.9)$$



(a) Entanglement entropy at the centre of chain for 100 sites.



(b) Entanglement entropy at the centre of chain for 200 sites. Note the sharp transition at near the critical point

Figure 3.10: Entanglement Entropy with respect to J/h_x

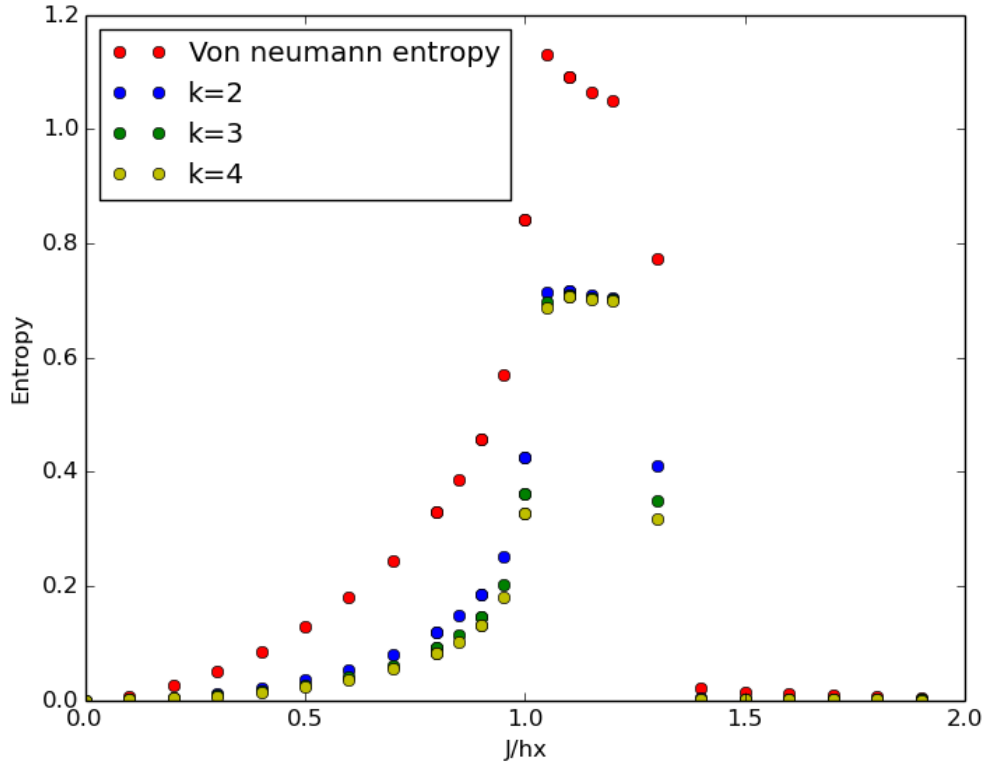


Figure 3.11: Von Neumann entropy and Rényi entropy for $k=2,3,4$ for 100 sites. When $k \rightarrow 1$ Rényi entropy collapses onto Von Neumann entanglement entropy

where $\hat{\rho}$ is the reduced density matrix and k can take values 2,3,4 and so on. For $\lim_{k \rightarrow 1} S_k(\rho)$ becomes Von Neumann Entanglement entropy. In Figure 3.11 we have plotted Rényi entropy for $k = 2,3,4$ and also Von Neumann entropy. The Rényi entropies are very close to one another and it can be seen that for $k = 2$ it lies at the top indicating that for k approaching 1 it is equal to the Von Neumann entropy.

Since we have seen how to calculate one point and two point correlation spin function using finite DMRG method we need to look into the variation of these with J/h_x . In Figure 3.12 we have plotted one point correlation function $\langle S_z \rangle$ at site 47 and site 96 for a lattice having 200 sites. We can see that both the functions show the exact behavior and they have a sharp transition from zero (paramagnetic phase) to about one (ferromagnetic phase) at the critical point $J/h_x = 1$.

Lastly we consider two point correlation between sites 81 and 97 and sites 51 and 97 on the lattice of 200 sites. The Figure 3.13 and 3.14. They have the same form as that of one point correlation near the critical point where they have a shape of anti-kink and kink curves. It is obvious from the graphs that the behavior of two point correlation functions also changes near the critical point indicating the phase transition. We can

also see that for TIM in two point correlation function changing length between the two sites doesn't change the form of graph much.

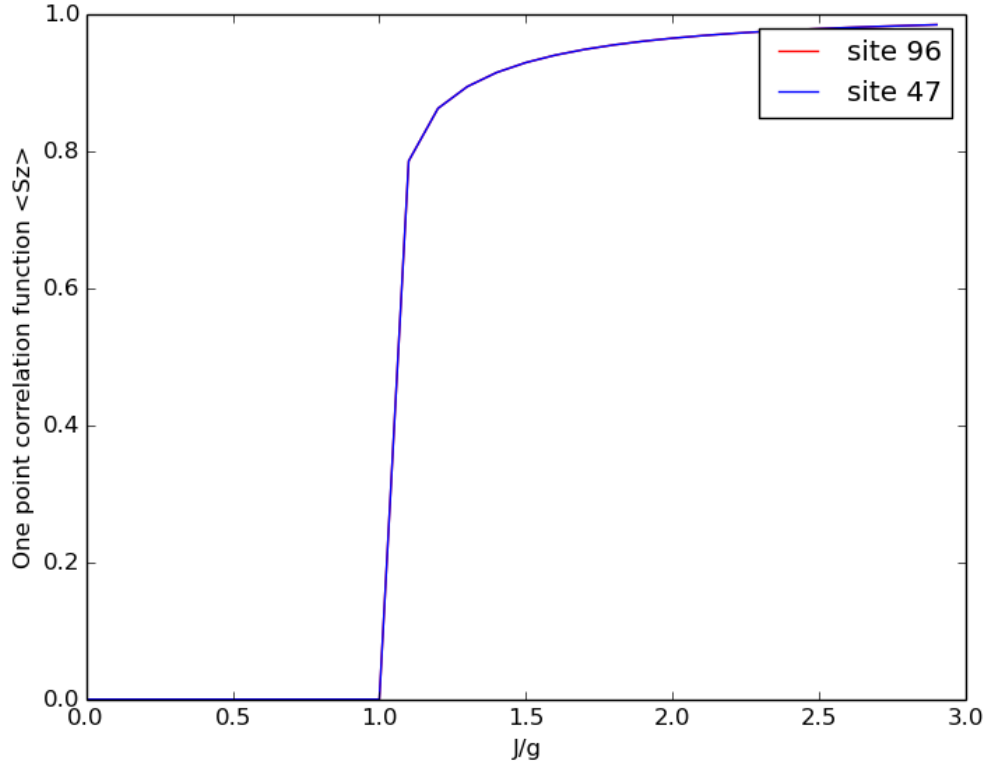


Figure 3.12: Plot of one point correlation function $\langle S_z \rangle$ with respect to J/h_x at site 96 and 47. $g = h_x = 1$

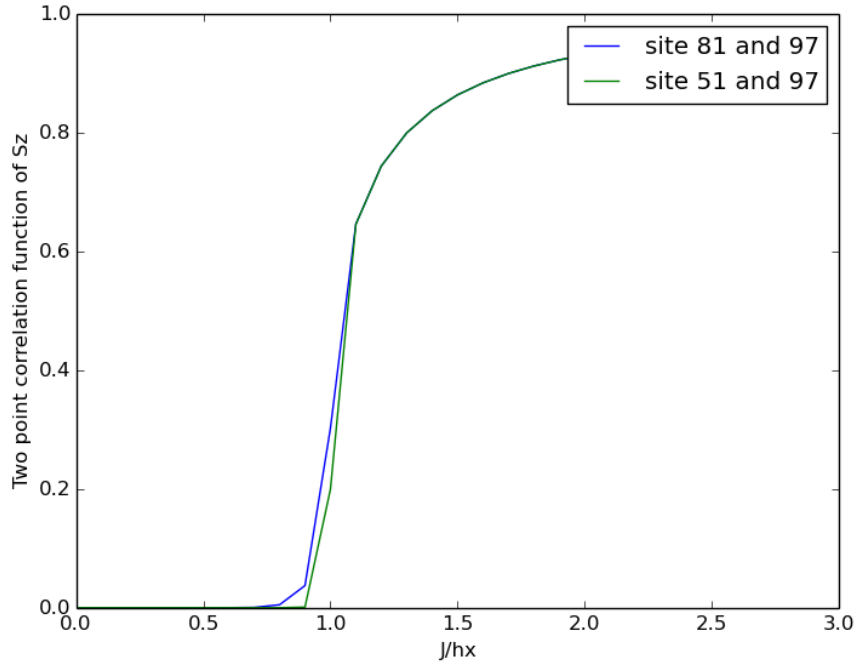


Figure 3.13: Two point correlation function of $\langle S_z \rangle$ for two different sites on a 200 sites lattice.

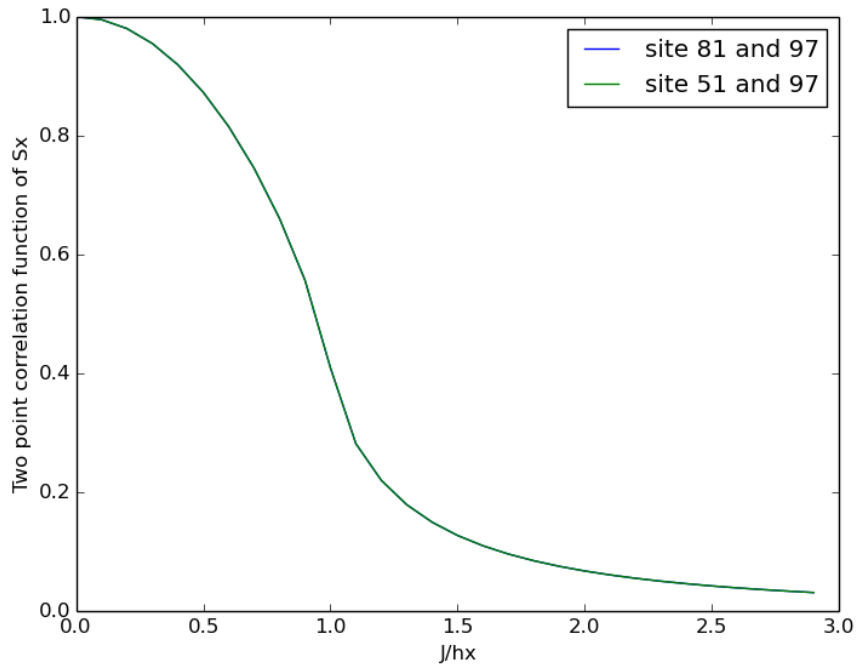


Figure 3.14: Two point correlation function of $\langle S_x \rangle$ for two different sites on a 200 sites lattice.

CHAPTER 4

XXZ Heisenberg Model

The Hamiltonian for anisotropic Heisenberg Model is given by

$$\hat{H} = \sum_i^{L-1} J \left(\hat{S}_i^x \hat{S}_{i+1}^x + \hat{S}_i^y \hat{S}_{i+1}^y \right) + J_z \sum_i^{L-1} \hat{S}_i^z \hat{S}_{i+1}^z \quad (4.1)$$

which in term of raising and lowering operators can be written as

$$\hat{H} = \sum_i^{L-1} \frac{J}{2} \hat{S}_i^+ \hat{S}_{i+1}^- + \frac{J}{2} \hat{S}_i^- \hat{S}_{i+1}^+ + J_z \hat{S}_i^z \hat{S}_{i+1}^z \quad (4.2)$$

where $\hat{S}^i = \frac{\hat{\sigma}^i}{2}$ and $\hat{\sigma}^i$ are the pauli operators defined previously. We can write the above Hamiltonian as

$$\hat{H} = J \left[\sum_i^{L-1} \frac{1}{2} \left(\hat{S}_i^+ \hat{S}_{i+1}^- + \hat{S}_i^- \hat{S}_{i+1}^+ \right) + \Delta \hat{S}_i^z \hat{S}_{i+1}^z \right] \quad (4.3)$$

We can put $J = 1$ for further calculations and Δ is called anisotropic coupling constant or anisotropy parameter. Letting this anisotropic coupling constant vary induces different ordering in the system, such that there are three phases characterised by: an antiferromagnetic region, an entirely critical paramagnetic region and ferromagnetic region. The various phases defined by Δ are

$\Delta > 1$	Ising Antiferromagnet	
$\Delta = 1$	Isotropic Antiferromagnet	
$-1 < \Delta < 1$	Paramagnet	(4.4)
$\Delta = -1$	Isotropic Ferromagnet	
$\Delta < -1$	Ferromagnet	

Later we will add external magnetic field to this model since the effect of a uniform magnetic field in the phase diagram of the XXZ chain is to extend the critical phase over a finite region. First we look at how ground state energy behaves when the anisotropy

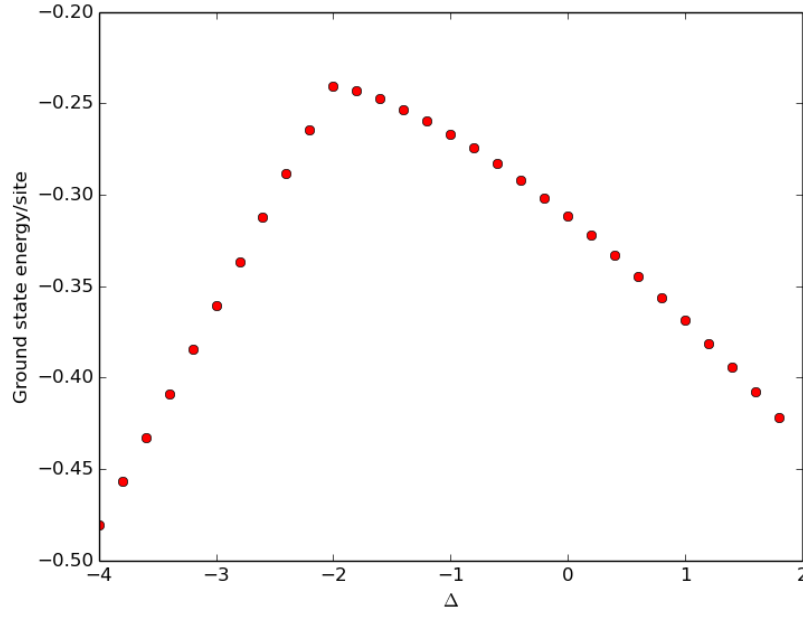


Figure 4.1: Ground state variation with Δ for a lattice having 50 sites. The reduced basis state number $m=40$

parameter Δ is varied. In Figure 4.1 we have plotted the variation for a lattice of 50 sites. Although this graph does not tell much but still from the change of slope in the graph one could see the hint of change in phase since the energy started decreasing abruptly after increasing for some values.

Just like for Transverse Ising Model we look at bipartite entanglement entropy for every bipartite splitting. That is we have plotted the entanglement entropy between block A and block B for each size of block A in finite size DMRG with total system size of 50 and 100 sites with $m = 40$. Following the same argument as before we can fit the above curve with logarithmic function of the form $y = A \log_2 x + k$ using the expression that relates the entanglement entropy to central charge and subsystem size given in (3.8). The central charge comes out to be 0.8115 for 50 sites and 0.6916 for 100 sites. As the size of the system goes to infinity this value of central charge should converge to a fixed point.

Lets look at the variation of mass gap with respect to the anisotropy parameter. It actually provides great insight in the nature of quantum phase transition. We know that for ferromagnetic region the mass gap is zero as can be seen in the Figure 4.3 where for $\Delta < -1$ we have a zero mass gap which starts having non zero value between $\Delta = -1$ to $\Delta = 1$ in which it increases linearly upto 1 where again there is a sharp transition which marks the anti-ferromagnetic region.

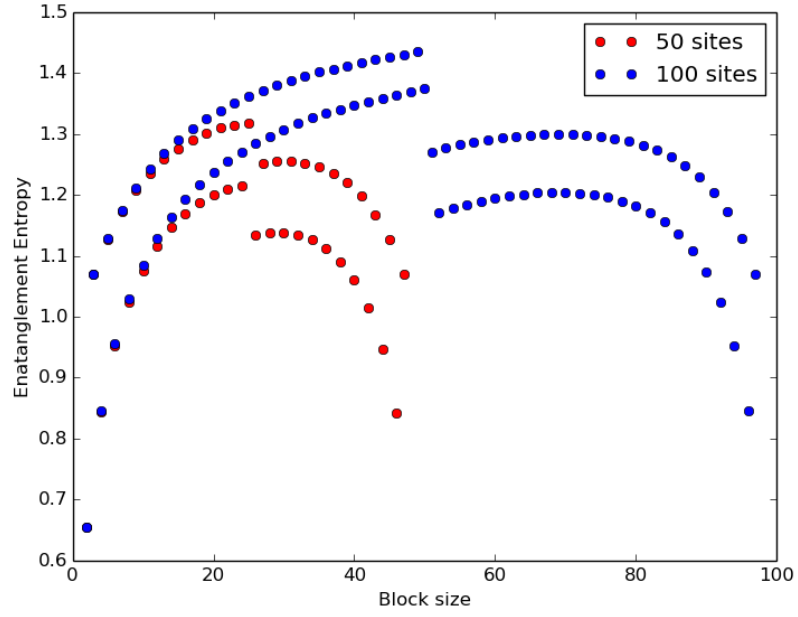


Figure 4.2: Plot of Entanglement Entropy at the centre of chain at every finite DMRG step vs the block size. The reduced basis states is $m=40$.

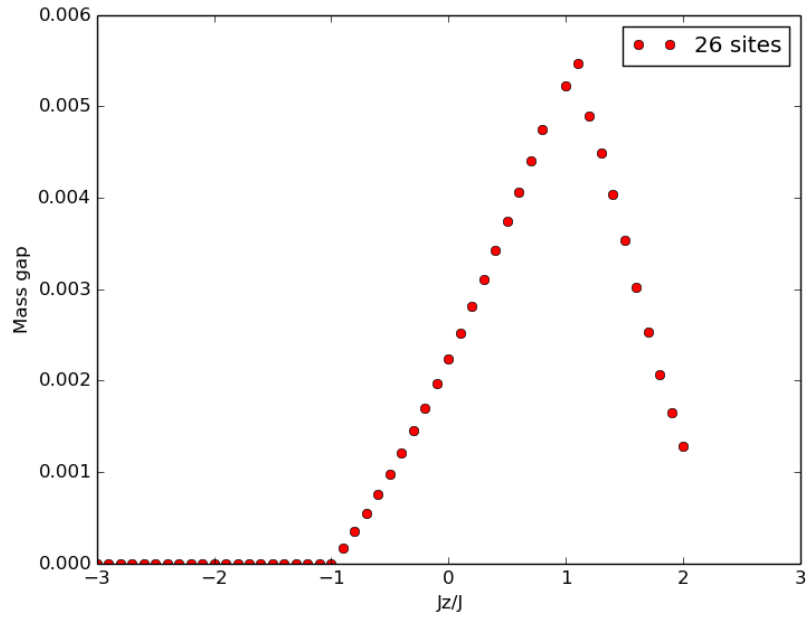


Figure 4.3: Plot for the variation of mass gap of Hiesenberg Model with Δ for a lattice of 26 sites. The reduced basis state number is $m=40$.

Since this model shows quantum phase transition from Ferromagnetism to paramagnetism and then Antiferromagnetism we need to two order parameter whose variation with anisotropy parameter we can study. For ferromagnetic state we have our usual order parameter $\frac{1}{N}\langle\sum_i S_i^z\rangle$ which is some of all the spins pointing in the \hat{z} direction. This follows the same behaviour as before i.e. this order parameter goes to zero in antiferromagnetic state which it should and is non zero for ferromagnetic phase. To study the nature of antiferromagnetic state we define a staggered order parameter given by $\frac{(-1)^i}{N}\langle\sum_i S_i^z\rangle$ where N is the total number of sites. This is just the sum of spin pointing in \hat{z} direction with the next neighbour spin pointing in opposite direction. We can try to guess its behaviour because we know that it should go to zero in ferromagnetic region and non zero in antiferromagnetic region. Under normal circumstances only the behavior of normal order parameter is obtained that too after applying an external field in longitudinal direction but for such field staggered order parameter does not show any variation. Therefore to see the transition happening in staggered order parameter not only do we need to apply magnetic field in longitudinal direction we need to apply a staggered magnetic field in the same direction. Reason is that we want a non zero value for our staggered order parameter. So what this staggered field will do is that it will try to align all the spin in staggered order parameter in one direction so that we get a non zero value for this order parameter in antiferromagnetic state. After testing various magnitude of external magnetic field we end up with values that give almost equal magnitude to both of our parameter. To our Hamiltonian in (4.3) we add two terms which are

$$-\sum_i^{L-1} h_z \hat{S}_i^z - h_{\text{stag}} \sum_i (-1)^i S_i^z \quad (4.5)$$

In Figure 4.4 as we can see the behaviour of order parameter for 100 sites is more accurate than for 50 sites because they actually go to zero when the other attains the maximum value. We can see transition happening around $\Delta = -1$ which is the start of the paramagnetic phase. The staggered order parameter gradually goes to zero and becomes completely constant (close to zero) in anti-ferromagnetic region. As the number of sites increases the portrayal of the actual behavior of the system becomes much more accurate. The values of h_x and h_{stag} is mentioned in the Figure 4.4

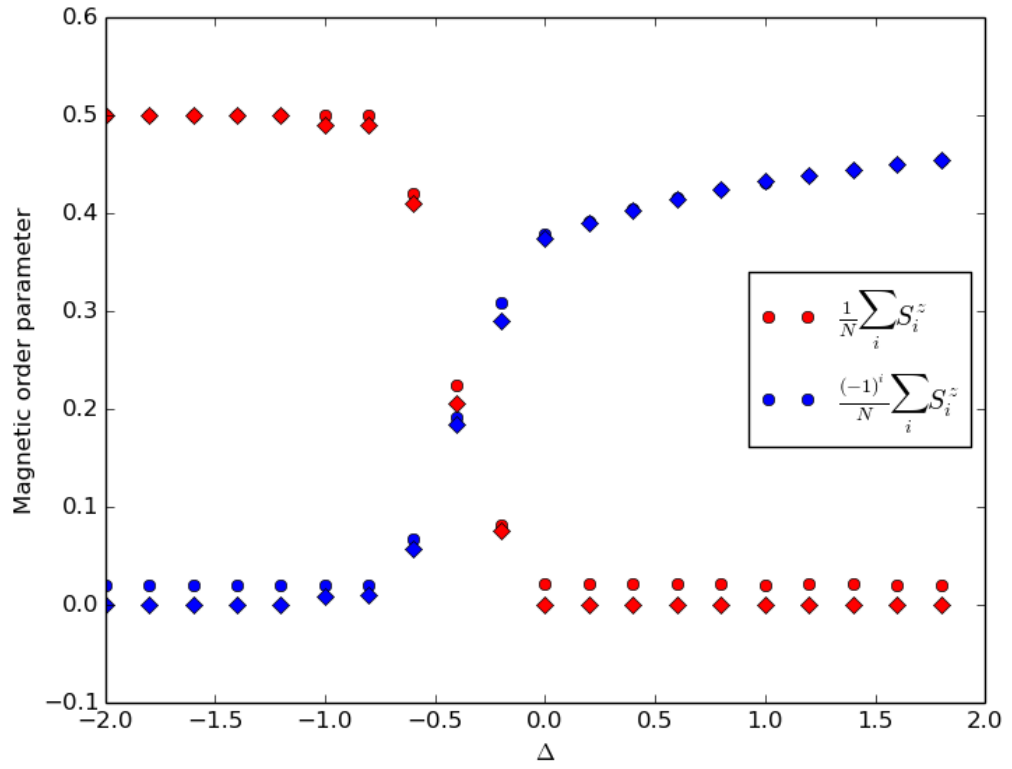


Figure 4.4: Order parameter variation with Δ for a lattice having 50 and 100 sites. The reduced basis state number is $m=40$. The red and blue circles are for 50 sites and diamonds are for 100 site. Here $h_z = h_{\text{stagg}} = 1.8$.

CHAPTER 5

Conclusions and Outlooks

In this thesis we studied the conceptual formulation of Density Matrix Renormalization Group (DMRG) and its differences and advantages over Wilson Renormalization Group. We explained the implementation of both finite and infinite system algorithm in order to find the ground state energy and its properties like bipartite entanglement entropy between system and environment block and mass gap of the system. We also discussed in detail about how to calculate observables like order parameter and correlation functions associated with ground state of the system using these algorithms.

We applied DMRG to 1D lattice systems like Transverse Ising Model and Heisenberg Model and by using DMRG algorithms the ground state energy was calculated in complete accordance with the theoretical result. While studying the behavior of various observables on external parameters like magnetic field (TIM) and anisotropy parameter (Heisenberg Model) we saw the evidences of quantum phase transition in both the models that were in agreement with the theoretical results. Such behaviour suggest that these observables can characterize quantum phase transition in an interacting model. In TIM we established two phases of the system which are ferromagnetic and paramagnetic, whereas in Heisenberg Model we saw the existence of a antiferromagnetic region, an entirely critical paramagnetic region and ferromagnetic region.

As a future work the DMRG algorithms can be used to solve more complicated interacting system such as Hubbard Model and can be extended to 2D systems which would require some modification since in present framework DMRG fails to predict ground state properly. We would also like to study the behaviour of block entropy in higher dimension. We can study the time dependent DMRG known as tDMRG which is used to study time dependent phenomena in various strongly correlating systems. One can also look into the relation between DMRG, quantum groups and conformal field theory.

REFERENCES

1. **Capraro, F.** and **C. Gros** (2002). The spin-1/2 anisotropic Heisenberg-chain in longitudinal and transversal magnetic fields: a DMRG study.
2. **Cardy, J.**, *Scaling and Renormalization in Statistical Physics*. Cambridge University Press, 1996.
3. **Cinnirella, A.** (2014). *Dynamics of the Heisenberg XXZ Model across the Ferromagnetic Transition*. Ph.D. thesis, University of Bologna, Bologna, Italy.
4. **Garrison, J. R.** and **R. V. Mishmash** (2013). Open source under the mit license. URL <https://github.com/simple-dmrg/simple-dmrg/>.
5. **Goldenfeld, N.**, *Lectures on Phase Transitions and the Renormalization Group*. Westview Press, 1992.
6. **Hallberg, K. A.** (2006). New Trends in Density Matrix Renormalization.
7. **Huang, K.**, *Statistical Mechanics*. John Wiley & Sons, 1987.
8. **Langari, A.** (1998). Phase diagram of the anti-ferromagnetic xxz model in the presence of an external magnetic field.
9. **Malvezzi, A. L.** (2003). An introduction to numerical methods in low-dimensional quantum systems.
10. **Schollwöck, U.** (2011). The density-matrix renormalization group in the age of matrix product state.
11. **Sei Suzuki, J.-i. I.** and **B. K. Chakrabarti**, *Quantum Ising Phases and Transitions in Transverse Ising Models*. Springer Berlin Heidelberg, 2013.
12. **White, S. R.** (1992). Density matrix formulation for quantum renormalization groups. *Physical Review Letters*, **69**(19), 4.
13. **White, S. R.** and **D. A. Huse** (1993). Numerical renormalization-group study of low lying eigenstates of antiferromagnetic s=1 heisenberg chain. *Physical Review Letters*, **48**(06), 10.
14. **White, S. R.** and **R. M. Noack** (1992). Real-space quantum renormalization groups. *Physical Review Letters*, **68**(24), 4.
15. **Wilson, K. G.** (1975). The renormalization group: critical phenomena and the kondo problem. *Reviews of Modern Physics*, **47**(04), 773–839.